2020

Development and validation of gene delivery methods for Crassostrea virginica

Adrienne N. Tracy
Colby College

Development and validation of gene delivery methods for *Crassostrea virginica*

Adrienne N. Tracy

Honors Thesis 2020

Colby College Department of Biology

Development and validation of gene delivery methods for *Crassostrea virginica*

An Honors Thesis

Presented to

The Faculty of The Department of Biology

Colby College

in partial fulfillment of the requirements for the

Degree of Bachelor of Arts with Honors

by

Adrienne N. Tracy

Waterville, ME

Advisor: José A. Fernández Robledo 

Reader: David R. Angelini _____

Reader: Ronald F. Peck 

Abstract

The Eastern oyster (*Crassostrea virginica*) is an important part of the East Coastal USA economy because aquaculture creates jobs. Sadly, the oysters are under constant threat due to increasing pollution, red tides, and diseases. Bivalves, and oysters in particular, are also becoming potential model organisms in medical research. With the sequencing of the oyster genome, scientists are focusing on deciphering the function of the predicted genes. However, the limited number of molecular and cellular tools available makes functional annotation of the genome challenging. A consistent, replicable gene delivery system needs to be developed to assess gene function and understand the oyster phenome. In this study, we adapted and furthered early methodologies for delivering DNA into oysters. We tested both chemical (dendrimers) and physical (electroporation) gene delivery into oyster hemocytes, *in vivo* and *in vitro,* using plasmids under CMV (*p*max-GFP, *p*CgVEGF-HA-GFP) and SV40 (*p*MLS-SV40-GFP) promoter control with green fluorescent protein (GFP) tagged genes. We observed GFP expression as early as 24 hours post transfection, in both *in vivo* and *in vitro* studies, using confocal microscopy. Indirect immunofluorescence analysis co-localized GFP with the anti-hemagglutinin antibodies in *C. virginica* hemocytes, expressing *C. gigas* vascular endothelial growth factor fused with hemagglutinin and GFP (*p*CgVEGF-HA-GFP). Transfection efficiency, using flow cytometry analysis, for *in vitro* and *in vivo* was 0.042% and 0.008% for *p*max-GFP, 0.061% and 0.01% for *p*MLS-GFP, and 0.071% and 0.009% for *p*CgVEGF-HA-IRES-GFP respectively. Here, we provide the basic methodology to understand the gene functions, and mechanisms that underlie oyster physiology and ecology, in order to annotate the oyster genome.

Table of Contents

Chapter 1: Introduction

Genetic studies on transfection of the Eastern oyster occurred as late as the early 2000s with limited success, but since then the oyster genome has been sequenced, bringing renewed interest in ways to deliver genetic material into oyster cells. This study aimed to use previous genetic methods to improve the genetic tools we have to study the Eastern oyster.

1.1 Ecological Impact

Oyster reefs are incredibly important ecosystems that help stem shoreline erosion, and eutrophication (Onorevole et al., 2018; Beck et al., 2011). The Eastern oyster (*Crassostrea*

virginica) has been proven to influence nitrogen cycling and enhance denitrification in sediments surrounding their reefs (Smyth et al., 2013; Bricker et al., 2018; Gàrate et al., 2019). As a result, oyster aquacultures have been proposed as a bioremediation technique to decrease nitrogen pollution that leads to eutrophication and hypoxia (Bricker et al., 2018; Li et al., 2020; Beck et al., 2011; Ray et al., 2019). Sadly, a large part of oyster reef coverage has been lost along the East Coast of the USA due to diseases and pollution, or a combination of both (Fernàndez Robledo et al., 2008; Zu Ermgassen et al., 2012; Beck et al., 2011; Dutertre et al., 2010; Caffrey et al., 2016; Smyth et al., 2013). Thus, bivalves are important to denitrifying microbial communities and have amazing potentials for mitigating nitrogen pollution and stabilizing fragile estuary nutrient cycles (Arfken et al., 2017; Smyth et al., 2013; Welsh et al., 2015).

While these organisms have the potential to help stem eutrophication in a future climate change scenario, they are also negatively impacted by climate change. Oysters require specific temperature ranges for gamete production, spawning, and development (Bernard et al., 2011; Chavez-Villalba et al., 2002; Fabioux et al., 2005; Mann, 1979). In addition, there is a correlation between oyster fecundity and phytoplankton availability (Bernard et al., 2011; Chavez-Villalba et al., 2002b; Auby & Maurer, 2004). With warming temperatures in the coastal waters of the Eastern US (Pershing et al., 2015), this means that oyster fecundities will change in the future. This could have very dire consequences to oyster reefs and their mitigation potentials.

1.2 Economic Impact

Bivalve aquaculture is a lucrative industry and has been valued at 16 billion dollars globally (Fernández-Robledo et al., 2018; Hartman et al., 2018). Furthermore, it is one of the

most sustainable aquaculture industries because its methods do not require additional food, vitamins, or antibiotics (Saravia et al., 2020; Smaal et al., 2019). One of the issues that comes along with bivalve aquaculture are harmful algae blooms that result in toxins, which can become concentrated and transferred to humans via bivalves. Additionally, bivalve aquaculture and wild populations alike face many diseases and parasites, leading to high mortality rates (Bucannan et al., 1992; Hartman et al., 2018). When these aquaculture populations decline it can cause serious economic damage to small aquaculture businesses (Dutertre et al., 2010; Saravia et al., 2020).

Perkinsus marinus, is a protozoan that causes 'Dermo' disease in Eastern oysters and has decimated populations of both wild and farmed oysters (Fernández Robledo et al., 2007; Yang et al., 2013). Annually, oyster populations can decrease by more than 50% due to *P. marinus* infections depending on the area (Buchannan et al., 1999; Proestou et al., 2019). Other diseases in the Eastern oyster are the parasite *Haplosporidium nelsoni,* which causes MSX, and the bacteria *Roseovarius crassostrea*, which causes juvenile oyster disease (JOD) (Yang et al., 2013; Paillard et al., 1996; Malloy et al., 2007; Buchannan et al., 1999). In *Crassostrea gigas*, the ostreid herpesvirus-1 has decimated the population of the Pacific oysters (King et al., 2019).

In order to combat these diseases, it is important to find disease resistant stocks to replenish the spats of wild reefs, as well as identify genes associated with disease resistance (Smaal et al., 2019; Yang et al., 2013). Currently, those in the aquaculture industry are using artificial selection to breed oysters with higher disease resistance, but this has had varying success (King et al., 2019; Yang et al., 2013). With more information on the genetics of the oyster, research could allow aquaculture farms to make more educated breeding decisions.

1.3 Medical Research

Bivalves have the potential to be model organisms for studying multiple facets of human health including microbiome turnover, innate immune systems, antibiotic alternatives, transmissible cancers, and bone and tissue regeneration. (Fernández Robledo et al., 2019; Smaal et al., 2019). For example, bivalves lack an adaptive immune system, which forces them to rely on their innate immune system to fight off disease (Fernández Robledo et al., 2019; Hartman et al., 2018). Furthermore, as they filter seawater through their pallial cavity and gills, this exposes their mantle and labial palp organs to the many microbes found in their ocean environment (Fernández Robledo et al., 2019). Studying this can help researchers understand the human innate immune system.

Mytilus edulis and *C. virginica* have the potential to lead to medical breakthroughs in bone regeneration. Bivalve shell production and formation goes through similar processes and uses similar proteins to those in human bone production and regeneration (Xu et al., 2019). Moreover, this research has led to the discovery that the oyster and mussel shell matrices can stimulate bone formation and regeneration in mouse, sheep and human osteoblast cells (Fernández Robledo et al., 2018).

Bivalves also have specific types of cancer that are important models for studying human cancer evolution. Bivalve transmissible neoplasia (BTN) is a leukemia-like cancer found in the hemolymph of several bivalve species (Carballal et al., 2015; Fernández Robledo et al., 2018). That being said, it is one of the few known cancers to be transmissible from animal to the next (Fernández Robledo et al., 2018). This makes the disease an incredible model system for

studying cancer resistance, tumor suppressor genes, and cancer evolution (Fernández Robledo et al., 2018).

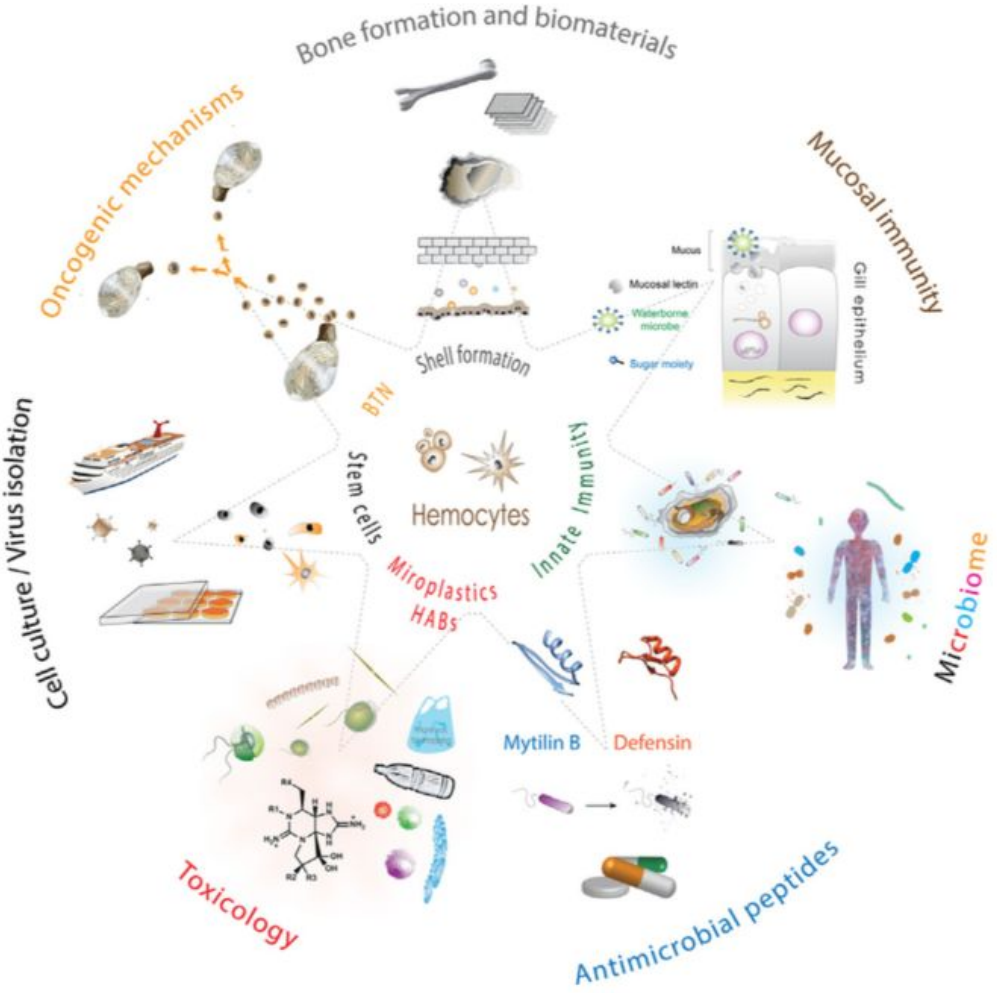

Figure 1. Schematic from Fernández Robledo et al., 2019 of possible biomedical applications of oyster research. Understanding oyster cells, immunity, shell formation, and genes will lead to many practical research applications in the biomedical research field as well as other fields (From: Fernández Robledo et al. 2019).

1.4 Cell Line Development

One of the major problems in exploring the oyster genome is the lack of oyster cell lines (Fernández Robledo et al., 2018; Boulo et al., 1996). Cells have been removed and cultured, but stop dividing after 24-72 hours (Richevich, 2011). These primary cultures generally last for about 2 months (Fernández-Robledo et al., 2018).

Cell lines are important to genetic research because they are less expensive than primary cell cultures, are genetically uniform, mitigate live animal testing, and allow researchers to reproduce experiments (Kaur & Dufour, 2012). No one has been able to maintain a marine bivalve cell line, and the closest cell line, phylogenetically speaking, is from a gastropod (Hansen, 1976; Rinkevich, 2011; Buchannan et al., 1999).

However, some genes have promise in stimulating oyster cells to replicate in culture. The small T antigen gene comes from simian virus 40 and causes rapid cell growth by accelerating and elongating the G1 phase of the cell growth cycle and delays the S phase (Krynska et al., 1998). The hTert gene codes for a ribonucleoprotein enzyme from human cancer cells that elongates the telomeres of chromosomes during DNA replication and allows the cell to live longer, or "immortalize" (Poole et al., 2002). By transfecting these genes into cells it may elongate the cell cycle enough to allow it to divide in culture.

1.5 Knowledge Gap

Since the oyster genome has been sequenced (Gomez-Chiarri, 2015), but not annotated for many promoters and coding regions, we need a standard reproducible methodology for transfecting oyster cells both *in vitro* and *in vivo* in order to annotate the genome. A annotated genome will allow us to utilize gene targeting technologies such as CRISPR/Cas9. In early *in*

vitro transfection experiments of oyster embryos, SuperFect (QIAGEN, Germantown, MD) was used as a chemical transfection agent that binds to plasmids and transports DNA through the cell's lipid bilayer membrane. However, high cell mortality was seen (Buchannan et al., 1999). Experiments with *in vivo* surf clam gamete transfection with a retroviral vector gene using electroporation found that 13-33% of gamete cells contained the transfected genes (Lu et al., 1996). Oyster embryos, larval stages, and live oysters, were transfected with a heterologous gene (cecropin B), but larval and embryonic cells had a 5-15% survival rate and only a third of the cells contained the transgene (Buchannan et al., 2001). For *in vivo* hemocytes transfected with chemical dendrimers, less than 5% contained the transfected heterologous genes (Buchannan et al., 1999). Since these transfection efficiencies are much higher in oyster embryos than in hemocytes (Buchannan et al., 1999), it is necessary to try to refine hemocyte transfection methods.

1.6 Choosing the Plasmids

We chose to look into plasmid vectors such as *p*max-GFP (Appendix A.), *p*MLS-SV40-GFP (Appendix B.), and *p*CgVEGF-HA-IRES-GFP for our experiments. GFP, or green fluorescent protein, is a protein isolated from the jelly, *Aequorea victoria* that fluoresces green when excited by a 488 nm laser (Buchannan et al., 1999). The GFP protein will allow us to see when and where the transfected or heterologous gene is expressed in the cell (Cheikh et al., 2017). In addition, the plasmid *p*CgVEGF-HA-IRES-GFP includes an HA antibody tag on the VEGF gene. If the plasmid is translated and transcribed in the hemocyte cell, we will see the GFP expression, but can also tag the GFP protein with primary and secondary antibodies. In

addition, we can add primary and secondary antibodies that bind to the HA protein. This secondary antibody fluoresces red, which means any cells with red and green fluorescence will demonstrate that the cell has successfully incorporated the plasmid, is actively translating the plasmid, and expressing the genes.

We chose plasmids with viral promoters SV40 or CMV, since viral promoters have been found to cause cells to transcribe viral DNA (Ansari et al., 1999). The SV40 promoter comes from the polyomavirus simian virus 40 and generally stimulates the production of the large and small tumor antigen, which causes a chronic infection in human organs and can infect human cells in culture (McNees et al., 2018; Keller and Alwine, 1984).The CMV promoter comes from the cytomegalovirus, which infects humans with DNA from the herpes virus, causes life long infection, and contributes to chronic immune activation (Maidji et al., 2017; Davis et al., 2017). Previous studies saw plasmid gene expression under the CMV and SV40 promoters in oyster embryo and hemocyte cells (Buchannan et al., 1999). By choosing these viral promoters we make it more likely that the cells will translate and transcribe plasmid genes once the plasmid is delivered to the cytoplasm.

We used the heterologous plasmids *p*max-GFP (Lonza, Walkersville, MD, USA), *p*CgVEGF-HA-IRES-GFP (Genbank, MT226487), and pMLS-GFP (Addgene #46919). All plasmids have a multiple cloning site (MCS) for C-terminus tagged with GFP of the gene to be tested. The *p*CgVEGF-HA-IRES-GFP has a CMV promoter and an HA antibody tagged vascular endothelial growth factor (VEGF). VEGF encodes a cell membrane protein that is used in development, regeneration, and biomineralization of shells and is a gene found in several marine invertebrates, including *Crassostrea virginica* (Ivanina et al., 2018). It also contains the internal

ribosomal entry site tagged to GFP. The *p*max-GFP also contains the CMV (cytomegalovirus) promoter driving GFP, with a C-terminus MCS region, in which future experiments can insert genes of interest. The *p*MLS-SV40-GFP contains the simian virus 40 (SV40) promoter driving GFP with a C-terminus MCS region. These plasmids allow us to test multiple different viral promoters and GFP tagged MCSs to see if one plasmid works more effectively than the others.

1.7 Choosing the Cells: Hemocytes

In order to test transfection in live oysters and oyster cells, we decided to transfect oyster hemocytes, or blood cells. Previous studies have transfected oyster and surf clam embryos, oyster larvae, and oyster gamete cells (Buchannan et al., 2001; Lu et al., 1996), however it is incredibly difficult to use embryonic cells, and gametes, since embryos must be dissociated to prevent further growth and live bivalves must be dissected for gametes. Instead, hemocytes are found in high abundance in the oyster adductor muscles, as muscle sinus is a non-lethal way to access the oyster circulatory system (Buchannan et al., 1999). This allows us to withdraw hemolymph easily and repeatedly from the adductor muscle using a hypodermic needle without killing the oyster.

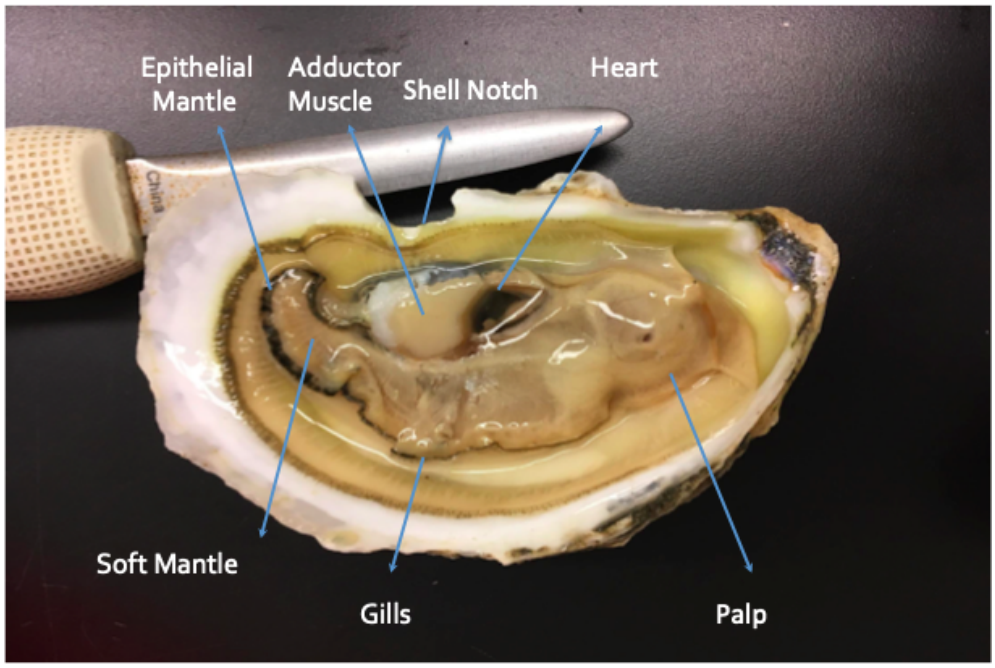

Figure 2. Dissected *Crassostrea virginica,* where the drilled oyster notch is labeled near the adductor muscle on the posterior dorsal side of the shell.

Hemocytes are generally classified into two groups: granulocytes and agranulocytes, whose distinctions are highly debated, but are generally distinguished through morphology (Fisher, 1986; McCormick-Ray & Howard, 1990; Cheng, 1975). Hemocytes are involved in the immune system response to invasive microorganisms through phagocytosis, clotting, and tissue repair (Fisher, 1986; Fernández-Robledo et al. 2018; Tripp, 1960). Since these cells are wide spread through the oyster's circulatory system and are constantly in use, they are the ideal cell source for developing the transfection methodology.

However, some of the cell functions can cause issues in the lab. For example, the cells form aggregates to form clots and heal tissues (Fisher, 1986). This means that if cells are exposed to transfection chemicals when they are in an aggregate, the chemical dendrimer won't

have equal contact with membranes of all the hemocytes. In order to avoid this, we added Alsever's solution to each mixture to break down the aggregate hemocyte formations (Bucahnnan et al., 1999; Bachere et al., 1988).

1.8 Methodology Background

We decided to attempt transfection of hemocytes in live oysters based on the easy access to cells without the need for long term cultures. While it is important to see if we can transfect live oysters to see gene function in the living animal, it is also important to be able to develop a system to transfect cells *in vitro*. This will allow scientists to decode gene function in individual cell types. However, since an oyster cell line hasn't been developed (Yoshino et al., 2013; Boulo et al. 1996), we still chose to use hemocytes for *in vitro* transfection. Again, this allowed for easy access to cells without killing the animal.

We decided to use polyamidoamine dendrimers that bind to DNA and transport it across the cell membrane (Dennig & Duncan, 2002; Buchannan et al., 1999; Qin et al., 1998). The dendrimers bind to DNA and form an activated DNA-dendrimer complex (Buchannan et al., 1999). The complex binds to the cell membrane and is uptaken through endocytosis into the endosome of the cell (Dennig & Duncan, 2002). From there, the complex is released into the cytosol and a small percentage of the complexes make it to the nucleus where the DNA is transcribed (Dennig & Duncan, 2002). This chemical transfection agent has been used in murine skin grafts, oyster embryos and live oysters (Buchannan et al., 1999; Qin et al., 1998).

While hemocytes are generally easier to work with, we used Alsever's solution to keep cells from clumping in primary culture (Buchannan et al., 1999; Bachere et al., 1988). By

keeping the cells from clumping, it increases cell contact with transfection dendrimers and allows for easier microscopic imaging and cell counting. Using these transfection methods (Buchannan et al., 1999; Lu et al., 1996) on *in vivo* and *in vitro* hemocytes will allow us to move the research of oyster genetics forward and begin to examine the oyster genome.

Chapter 2: Method Development

2.1 In Vivo Transfection Methods

The *in vivo* experimental methods were adapted from Buchannan et al., 1999, 2001, where the transfection solution was injected into the adductor muscle of the live oyster in the hopes that it would reach hemocytes in the blood vessels. Live oysters from the Damariscotta River Estuary (ME, USA) were stored in a 10-gallon bucket incubated between 12 and 16˚C, containing air bubblers. They were kept in sand filtered seawater from the Damariscotta River Estuary (ME, USA). The sand filtration removed large particles, and zooplankton, but allowed phytoplankton to pass through filters, serving as food for the oysters. The water was changed and the buckets were cleaned once a week.

The oyster's shells were notched on the posterior dorsal side of the shell for easy access to the dorsal adductor muscle (Buchannan et al., 2001; Larson et al., 1989). A Dremel (Racine, Wisconsin, USA) was used to shave down the edge of the shell of each oyster until an opening formed. Each opening was tested with a 19G needle (BD Microlance) to ensure that it was large enough.

Oyster "serum" was prepared to increase the probability that oysters would accept transfection chemicals into their circulatory system following the methods of Buchannan et al.,

1999, Chu et al., 1993, and Larson et al., 1989. Hemolymph was extracted from the posterior dorsal adductor muscle by taking 100 µL of Alsever's (Alpha Aesar, Tewksbury, MA) in a 1mL/cc syringe (Global) with a 19G needle. Approximately 900µL of hemolymph was extracted from a few oysters. The hemolymph was centrifuged at 1,000 rpm, 4°C for 10 minutes. The pellet of hemocytes was discarded and the hemolymph supernatant was recovered and filter sterilized with a 0.22 µm Supor membrane filter (Pal Corporation, CA, USA). The oyster serum from each oyster was combined and frozen for later use.

The plasmids *p*max-GFP (Lonza, Benicia, CA, USA), *p*MLS-GFP (Lonza), and *p*CgVFGF-HA-IRES-GFP (GenBank, MT226487) were dried in 5 µg concentrations and put into individual 2 mL Eppendorf Tubes. The plasmid tubes were dried using a Svant 120 Speedvac Concentrator (Thermo Scientific, Waltham, MA, USA), on the auto setting with heat. Next, 5µg of plasmid was resuspended in 33.0 µL of filter sterilized oyster serum. Then 67.0 µL SuperFect (Quiagen, Germantown, MD, USA) was added to the solution for a total volume of 100µL and a ratio or 1:2. The solution was injected into the oyster almost immediately after being added to the plasmid DNA because SuperFect can degrade DNA over time.

Three replicate oysters were transfected with each plasmid. There were three control oysters containing either 100 µL of filter sterilized oyster serum to see if mixing hemolymph from different oysters causes negative effects, a mixture of 67µL Superfect and 33 µL of oyster serum to see if SuperFect alone causes fluorescence, or 5 µg *p*max-GFP plasmid DNA resuspended in 33 µL oyster serum and an additional 67 µL of oyster serum to see if DNA alone causes fluorescence. This gave an oyster serum control, a SuperFect control, and a plasmid control.

After the transfection solution was injected into the oysters, they sat out in open air for two hours before being returned to the buckets of seawater to allow less dilution of the transfection solution before activated dendrimer uptake into the cells. Control oysters and transfected oysters were kept in separate buckets to avoid the possibility of exposing control oysters to transfection solutions.

Hemolymph (100 µL Alsever's (Alpha Aesar) and 200 µL hemolymph) was extracted from each transfected oyster replicate and each control at approximately 1, 3, and 8 days post transfection. The hemocyte cells were checked for fluorescence using the flow cytometry (ZE5, BioRad, Hercules, CA, USA) and confocal microscopy (LSM-700, Carl Zeiss, Pleasanton, CA, USA).

2.2 In Vitro Transfection Methods

The *in vitro* experimental methods were adapted from Lu et al., 1996 and Buchannan et al., 1999, and 2001, where hemocytes were removed from the oyster hemolymph and transfected in primary culture. For the *in vitro* experiments, approximately 300 µL of oyster hemolymph was withdrawn from individual oysters and kept on ice. Each oyster's hemolymph was kept separate. Next, 5µg of the plasmid was dried in the Svant 120 Speedvac Concentrator in individual Eppendorf tubes on the auto setting with heat. The 5 µg of each dried plasmid was re-suspended in 33 µL in filter sterilized (0.22 µm) oyster hemolymph. Then, 67 µl of Superfect was added for a total volume of 100 µL and a 1:2 ratio of plasmid to Superfect. The cells were recovered from the 300µL of extracted hemolymph from individual oysters through centrifugation at 1,000 rpm, 4°C for 10 minutes and put into a Cyto-One 12-well plate (USA Scientific, Ucala, FL, USA)

containing 1mL Alsever's. The 100µL of transfection solution was added to each well, and wells were resuspended to mix the transfection solution with cells. The plate was incubated at 12-16˚C. Oyster hemolymph was extracted to check for fluorescence using the flow cytometer (BioRad ZE5) and confocal microscope (Zeiss LSM-500) at 1, 3, and 8 days after transfection.

2.3 Electroporation Methods

Approximately 500 µL - 1000 µL of oyster hemolymph was withdrawn from each oyster and centrifuged at 1,000 rpm, 4°C for 10 minutes. The variation in hemolymph extraction volume was due to some oysters' resistance to hemolymph extraction. The supernatant was removed and the hemocytes were resuspended in 1 mL of hemolymph serum.

The electroporation techniques came from the Lonza Amaxa Human Monocyte Nucleofector Kit program Y-01. The 5 µg of plasmid was resuspended in a volume of 100 µL electroporation solution, Buffer V (Lonza, Benecia, CA, USA). The solution was added to the 1 mL of hemolymph and immediately transferred to an electroporation cuvette (Lonza, Benecia, CA, USA) and electroporated (Lonza, Benecia, CA, USA) using the Y-01 program that is used on Mammalian Blood Cells. After electroporation the solution containing the transfected cells was placed in a 12-well plate in 1 mL of the combined filter sterilized (0.22 µm) hemolymph serum and incubated at 12-16˚C.

Chapter 3: Method Quantification and Qualification

3.1 Confocal Analysis

At days 1, 3, and 8 post transfection, cells from each transfection method were prepared for confocal microscopy. Approximately 200 µL of hemolymph and 100µL of Alsever's were withdrawn from each *in vivo* transfected oyster and put in a 4-well confocal plate. For the *in vitro* cells, an unfiltered pipette tip was burned with a Bunsen burner to seal and then scraped on the bottom of the well to dislodge cells that had stuck to the bottom. Then the cells were resuspended before removing 100 µL of well solution and 100 µL of Alsever's was put into the 4-well confocal plate. The baseline auto-fluorescence was measured using the control hemolymph. Gates were defined at the levels of autofluorescence seen in many of the control oysters, so that only fluorescence at a higher intensity from controls would be detected. Cells with green fluorescence were imaged at 200x magnification and then saved for later image analysis.

3.2 Cell Profiler Image Analysis

Cell profiler image analysis software version 3.1.8 (Jones, 2008) was used in order to compare fluorescent intensity and fluorescent area between different transfected hemocyte cells imaged using the confocal microscope. This software allowed us to quantitatively compare images from the different methods used. A pipeline for analysis was used that first takes images and turns them to black and white to measure light intensity differences. Then the images were manually cropped around fluorescent cells, which appear as bright white in the software. The software identified the primary objects, identifying objects from 1 to 100,000-pixel units. The software then identified the size and shape of those features, with the Zernike Features included, and measured object intensity in relative fluorescent units (RFUs) (Figure 3). The image analysis data was saved to a spreadsheet and statistically analyzed in R (R Core Team, 2018) using the

ggplot2 (Wickham, 2016), plotly (Seivert, 2018), data.table (Dowle & Srinivasan, 2018), tidyr (Wickham & Henry, 2018), dplyr (Wickham et al., 2018), and R Color Brewer (Neuwirth, 2014).

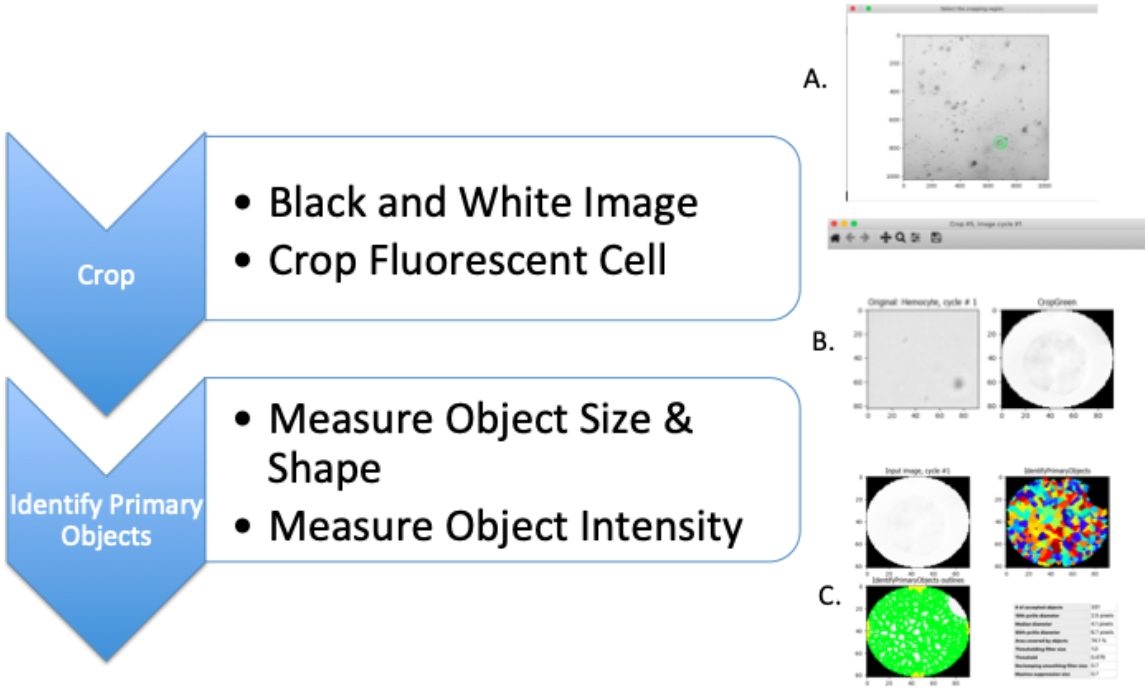

Figure 3. Schematic of Cell Profiler Image Analysis 3.1.8 (Jones, 2008) Pipline. Confocal Images are cropped around fluoresenct cells (A & B). Then primary objects are identified by the software and measured for object size, shape and fluorescent intensity (RFUs) (C).

3.3 Flow Cytometry

At approximately days 1, 3, and 8 post transfection, cells from each transfection method were prepared for flow cytometry. Approximately 200µL of hemolymph and 100µL of Alsever's were withdrawn from each *in vivo* transfected oyster and put in 1.5 mL Eppendorf Tubes on ice. For the *in vitro* cells, a pipette tip was burned with a Bunsen burner and then used to dislodge cells that had stuck to the bottom. Then 100µL of well solution and 100µL of Alsever's was put

in 1.5 mL Eppendorf Tubes on ice. The samples were filtered with 40µm cell strainers to get rid of hemocyte clumps.

The samples were put in the BioRad ZE5 flow cytometer and the baseline was set up with 1 mL of control hemolymph. Gates were shifted to fit the control sample's background autofluorescence. A 488 nm laser light was used to excite cells containing green fluorescence. This determined transfection efficiency by counting total cells and the number of cells expressing GFP. Gates were made based on side scatter area 488 nm versus forward scatter area 488 nm, in order to isolate granulocyte and agranulocyte sizes of hemocytes. Then forward scatter area 488 nm versus forward scatter height 488 nm, were set up to isolate the singlet versus doublet populations. Then green fluorescence 488 nm log area versus red fluorescence 640 nm logheight gates were set up to isolate hemocytes with GFP, instead of phytoplankton or bacteria with chlorophyll-a present (Figure 3). The flow cytometer withdrew the first 150µL of each sample in order to get approximately 100,000 cells. The baseline hemocytes were compared to transfected hemocytes to determine the number of GFP transfected cells. Transfection efficiencies were calculated from the number of fluorescent cells divided by the total number of hemocytes.

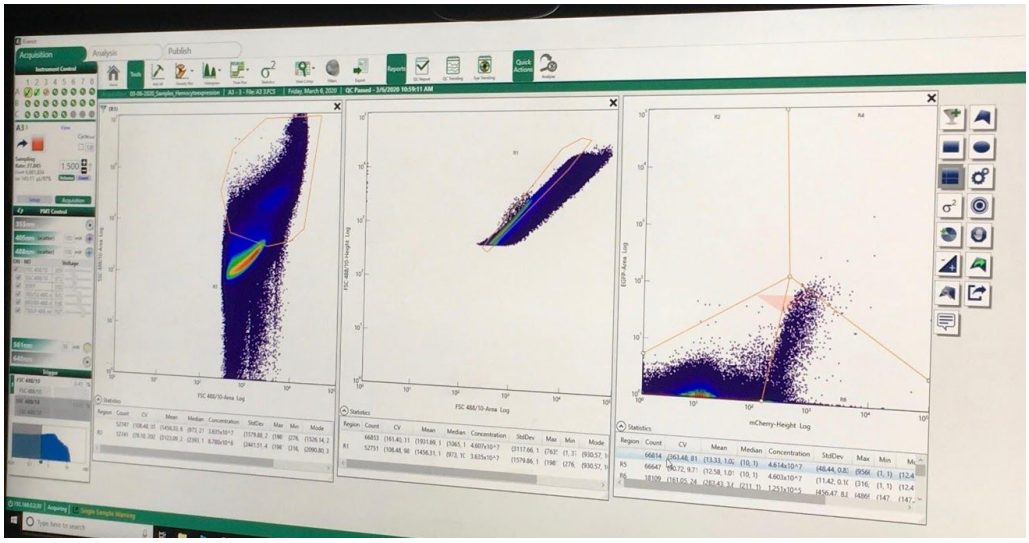

A.

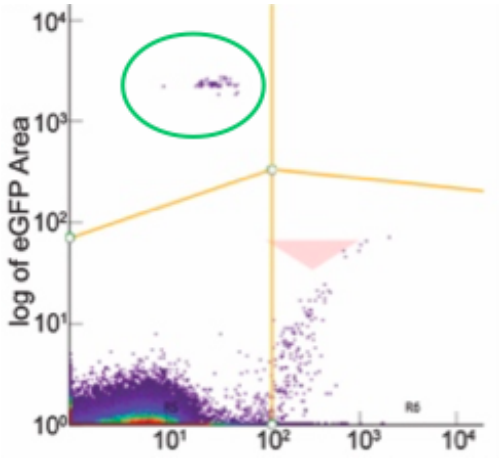

B.

Figure 4. Flow cytometer (BioRAD ZE5) gates to isolate GFP expressing cells. (A.) Gate 1 is SS Area 488 versus FS Area 488. Gate 2 is FS Area 488 versus FS Height 488. Gate 3 is EGFP Area Log (Green Fluorescence) versus mCherry Height Log (Red Fluorescence). (B.) Gate 3 is EGFP Area Log (Green Fluorescence) versus mCherry Height Log (Red Fluorescence) where gate R2 (circled in green) is the population of cells expressing GFP, and the R4 is the population

of cells expressing both green fluorescence and red fluorescence. These cells likely contain chlorophyll-a and could be contamination from phytoplankton filtered in by the oysters.

3.4 Immunofluorescent Assay

Immunofluorescent assays (IFA) were performed on the transfected hemocytes to determine the expression of GFP and HA proteins in transfected cells, following similar methods to those of Noël et al. 1996 and Pipe 1990. IFA was done for the expression of GFP for cells transfected with *p*MLS-SV40-GFP, *p*max-GFP, and *p*CgVEGF-HA-IRES-GFP. It was also done for the expression of VEGF-HA in the cells transfected with *p*CgVEGF-HA-IRES-GFP. The hemocyte cells were first incubated on ice to allow them to adhere to the NunC Lab-Tek chambered coverglass (Thermo Scientific, Waltham, MA, USA) of the confocal plate wells. The cells were washed with PBS three times and then fixed with 3% paraformaldehyde. The fixed cells were kept at 4˚C until assays were prepared.

3.4.1 HA Antibody Tagging - Colocalization Study

Cells were washed with PBS x3 to remove excess paraformaldehyde. For the plasmid pCgVFGF-HA-IRES-GFP a colocalization was done using primary rabbit monoclonal anti-HA antibodies (Cell signaling, Danvers, MA, USA). Anti-HA primary antibodies diluted at 1:5,000 were added to the hemocytes and were incubated for 1 hour at 37˚C. They were washed three times with PBS to remove any unbound antibodies. Anti-HA antibody hemocytes were incubated with conjugated anti-IgG rabbit antibody (Molecular Probes, Eugene, OR, USA). The binding of these antibodies confirmed expression of HA genes and showed localization of the expression

within the cells. After incubations of the secondary anti-IgG rabbit antibody, cells were washed three times with PBS to remove unbound secondary antibodies. Pre-immunized rabbit serum was used as a control and cells were analyzed under the confocal microscope, with lasers of 488, 555, and 568 nm, to determine the presence of antibodies.

3.4.2 GFP Antibody Tagging - Colocalization Study

Cells were washed with PBS x3 to remove excess paraformaldehyde. For all plasmids a colocalization was done using primary mouse monoclonal anti-GFP antibodies. Anti-GFP primary antibodies diluted at 1:10,000 were added to the hemocytes and were incubated for 1 hour at 37˚C. Cells were washed with PBS x3 to remove any unbound antibodies. Anti-HA antibody hemocytes were incubated with conjugated IgG-mouse antibody (Southern Biotech, Birmingham, AL, USA). The binding of these antibodies confirmed expression of GFP genes and showed localization of the expression within the cells. After incubations of the secondary IgG-mouse antibody, cells were washed three times with PBS to remove any unbound secondary antibodies. ProLong Diamond Antifade mountant supplemented with 4', 6-diamidino-2-phenylindole (DAPI) (Molecular Probes, Eugene, OR) was used to mount the coverglass onto the slide. Pre-immunized mouse serum was used as a control and cells were analyzed under the confocal microscope, with lasers of 488, 555, and 568 nm, were used to determine the presence of antibodies.

3.6 Data Analysis

The data from the flow cytometry and cell profiler was analyzed in R (R Core Team, 2018). The means and standard deviations of GFP efficiency and fluorescence were calculated using the dplyr (Wickham et al., 2018) package. Plots were done using the ggplot2 (Wickham, 2016), plotly (Seivert, 2018), and R Color Brewer (Neuwirth, 2014) packages. Statistical analysis was done using data.table (Dowle & Srinivasan, 2018), tidyr (Wickham & Henry, 2018) and Median Polish Analysis (Klawonn et. al, 2013).

Our data didn't fit the assumptions needed for an ANOVA due to a non-normal data distribution and low sample numbers. Instead, the median polish statistical analysis was used as a non-parametric data analysis tool (Klawonn et. al, 2013) to find the effect strength of each categorical variable on the transfection efficiency data. This allowed later experiments to focus on the *p*CgVFGF-HA-IRES-GFP plasmid vector, which had stronger effects. Non-parametric Wilcoxon tests were run between plasmids and controls to test if plasmids showed higher transfection efficiencies than control groups. The mean, standard deviation and standard error of the GFP intensity of each plasmid from the cell profiler results were found using the dyplr package (Wickham et al., 2018). ANOVAs were run on the confocal cell profiler results because there was a sample size of more than thirty images, despite the data being non-parametric.

Chapter 4: Results

4.1 In Vivo and In Vitro Results

Confocal imagery showed fluorescent green hemocytes with each transfected plasmid, as well as each method (*in vivo, in vitro*, and electroporation), only 24 hours post transfection (Figure 4). There were several fluorescent cells seen under each plasmid and each method. The

fluorescence in cells lasted for 9 days post transfection and began as early as 24 hours post transfection. However, it is unknown how long the gene expression occurs past 9 days.

Confocal imagery and cell profiler results show that there is a wide range of green fluorescent intensities in hemocytes transfected with each plasmid and within each control. That being said, there were higher intensities seen in *p*max-GFP transfected cells (Figure 5). The *p*MLS-GFP plasmid exhibited higher fluorescence in the *in vitro* experiments, but not the *in vivo* experiments. The control groups of oyster serum, plasmid controls, and SuperFect controls also exhibited high fluorescence due to the hemocyte's tendency to autofluoresce.

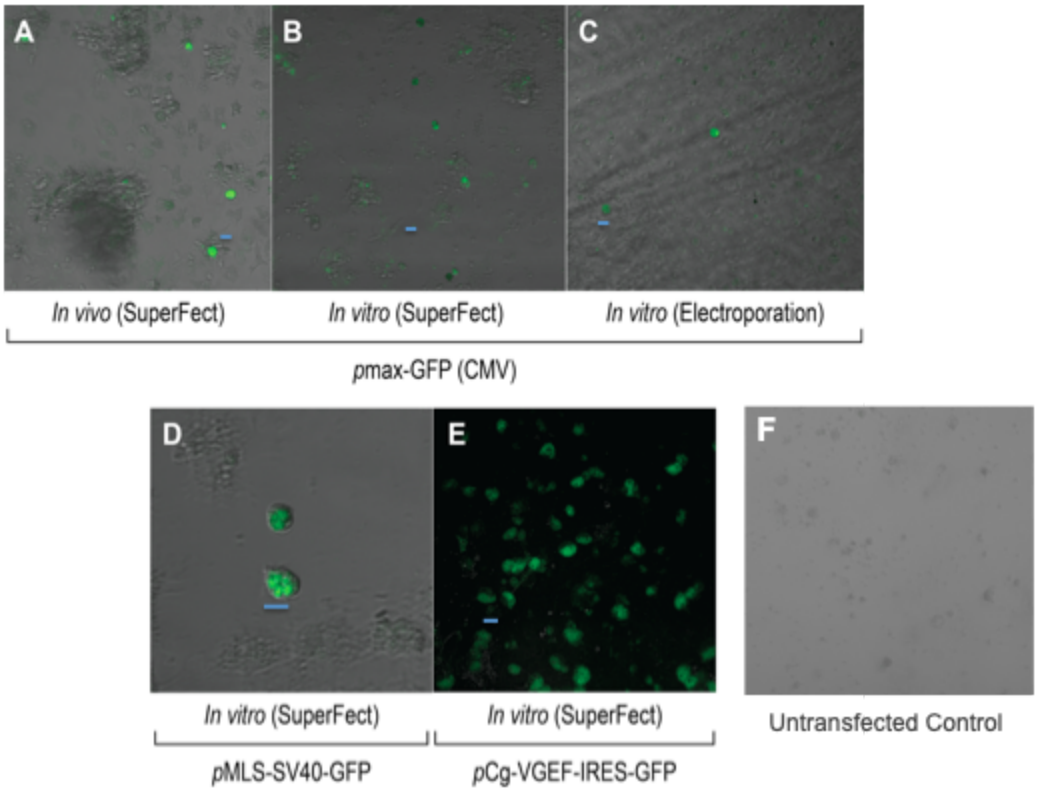

Figure 5. Successful expression of GFP genes *in vitro* and *in vivo* in primary cultured Eastern oyster (*C. virginica*) hemocytes. **A**. *p*maxGFP *in vivo* with SuperFect. **B**. *p*maxGFP *in vitro* with SuperFect. **C.** *p*maxGFP *in vitro* with electroporation. **D.** *p*MLS-SV40-EGFP *in vitro* with SuperFect. **E.** *p*CgVEGF-HA-IRES-GFP *in vitro* with SuperFect. **F.** Confocal images of control (untransfected) hemocyte cells. Scale bar, in blue, is 10 µm.

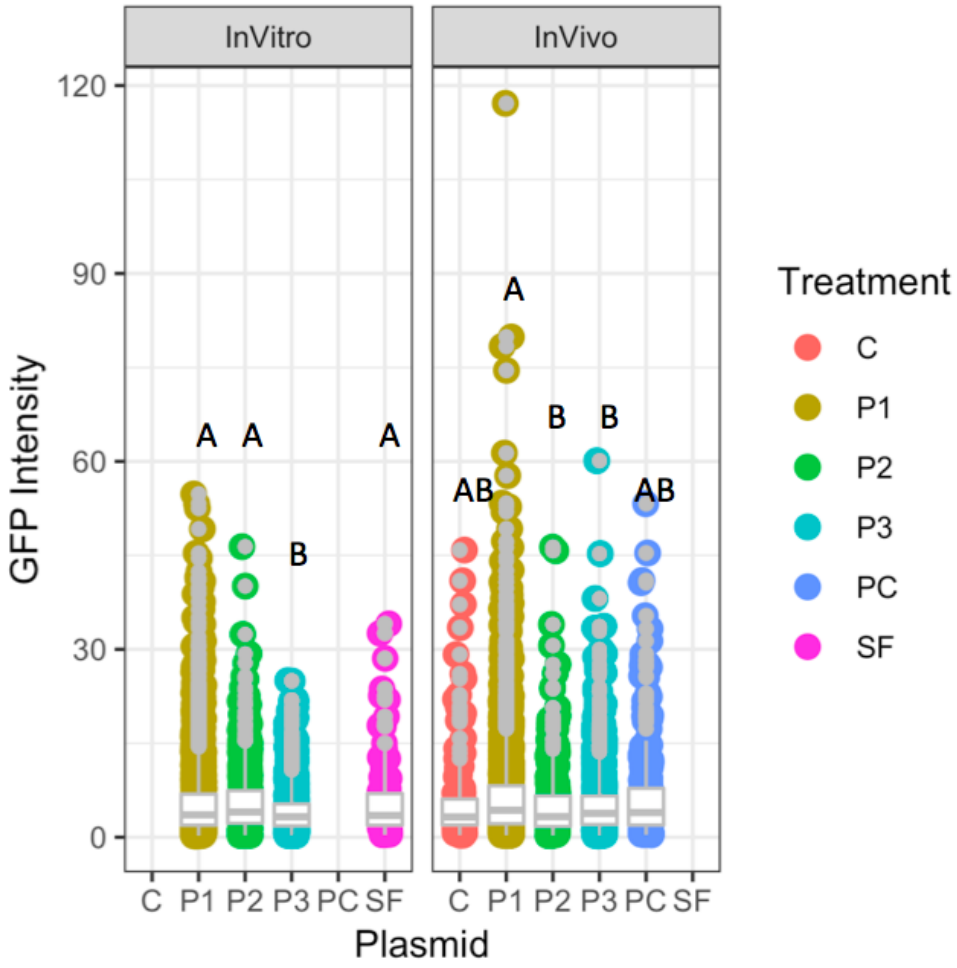

Figure 6. Confocal image analysis of fluorescent intensity from cells expressing GFP from 3 independent plasmids using Cell Profiler software. Where, P1 = *p*max-GFP, P2 = *p*MLS-GFP, P3 = *p*CgVEGF-HA-IRES-GFP, C = transfection serum control, PC = plasmid control, SF =

SuperFect control. ANOVAs were run with a Tukey HSD, giving a p-value of $p < 0.01$ for both *in vitro* and *in vivo*. The statistically significant p-values (Tukey tests) of GFP intensity are noted with either A or B. Significant p-values are $p < 0.05$ with $n = 4000$.

IFA analysis showed that there was GFP and VEGF-HA translation in hemocyte cells from *p*max-GFP and *p*CgVEGF-HA-IRES-GFP transfections respectively. GFP IFA showed the colocalization of green fluorescence and red fluorescence in the cytoplasm of the hemocyte cells after confocal microscope imaging (Figure 6). The IFA demonstrates that the cells are translating the GFP in the *p*CgVEGF-HA-IRES-GFP and *p*max-GFP plasmids given that control cells do not show colocalization. Thus, we can assume that cells transfected with different plasmids, exhibiting similar green fluorescence under the confocal microscope, are also expressing and translating plasmid genes.

The hemocytes transfected with *p*CgVEGF-HA-IRES-GFP exhibited colocalization of the red fluorescent anti-HA antibody and the green fluorescence of GFP (Figure 7). This shows that the cells are expressing the GFP in the *p*CgVEGF-HA-IRES-GFP. Since HA is tagged to the VEGF gene, that means that the hemocyte is also expressing the VEGF gene.

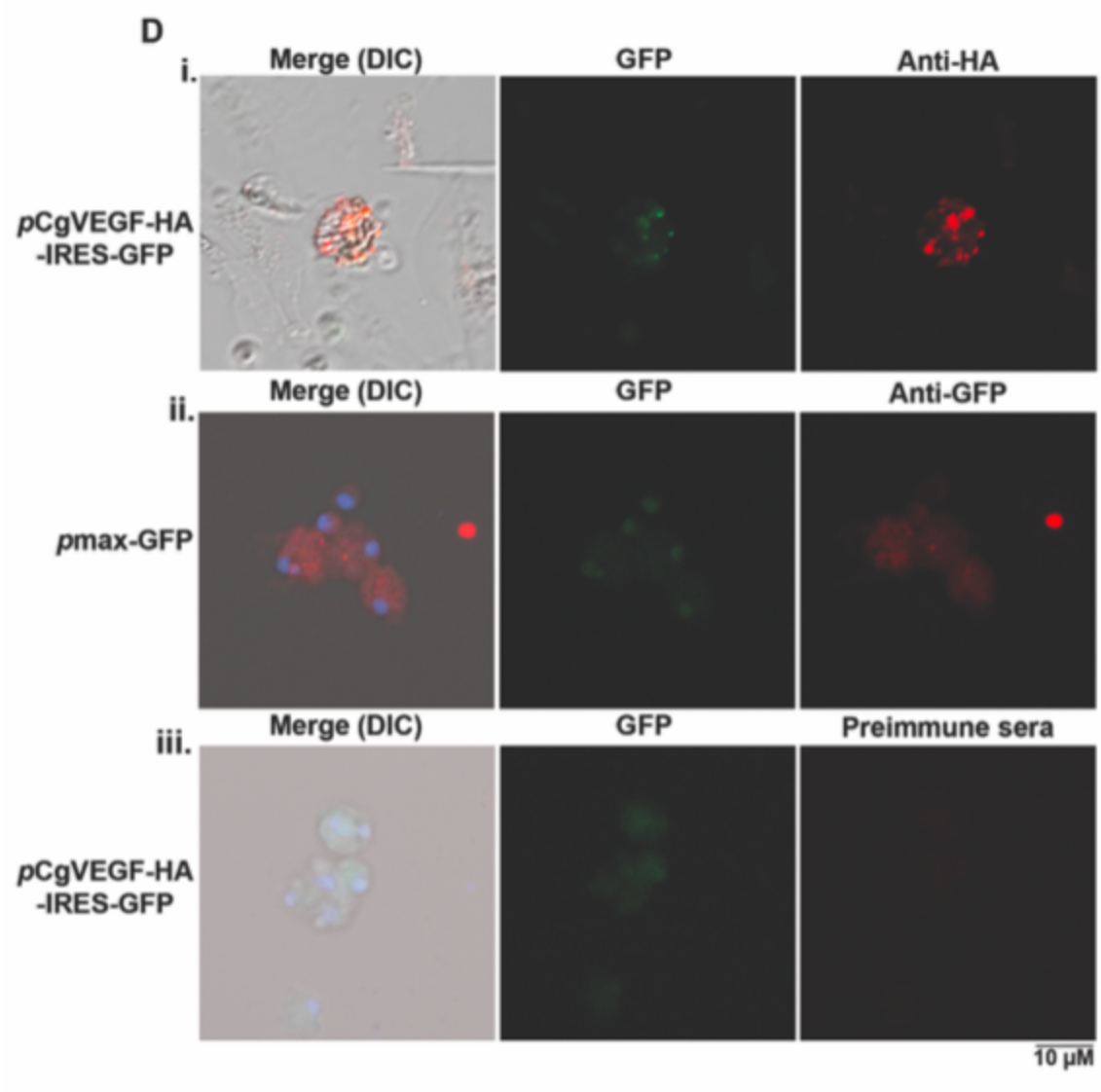

Figure 7. **(i)** Colocalization of GFP (green fluorescence) and anti-HA (red fluorescence) where green and red fluorescence were colocalized in the cytoplasm of the *p*CgVEGF-HA-IRES-GFP transfected hemocytes. **(ii)** Colocalization of GFP (green fluorescence) and anti-GFP (red fluorescence) in *p*max-GFP transfected hemocytes, where green and red fluorescence was seen in the same places in the cytoplasm of the hemocytes. DAPI staining in blue shows the nucleus of the hemocytes. **(iii)** Control IFA with *p*CgVEGF-HA-IRES-GFP transfected hemocytes and preimmune sera treatment with no colocalization seen. Scale bar at 10 µm.

Flow cytometry quantified transfection efficiencies were found to be generally lower than 0.1% (Table 1). The efficiencies showed that a small population of the cells were successfully transfected with the plasmids. However, there were some differences amongst plasmids and methods. The highest transfection efficiencies were seen *in vitro* in *p*CgVEGF-HA-IRES-GFP (Figure 8). However, there was no statistical significance between plasmids and controls, with a p-value of $p < 0.4$ (Wilcoxon non-parametric test), due to the fact that each sample had a large variation in the number of fluorescent cells (Figure 8). The plasmid control and SuperFect controls showed very high transfection efficiencies compared to samples with transfected plasmids (Table 1).

Table 1. Mean transfection efficiencies (% #fluorescent cells/sample) of fluorescent cells in a transfected sample quantified with a flow cytometer where none are statistically significant, with a p-value of $p < 0.4$ *in vitro* and *in vivo*, n=3 (Wilcoxon non-parametric test). Data came from three experiments averaged together with three replicate oysters or wells from each plasmid.

	In vitro	*In vivo*
Control	0.023	0.009
*p*max-GFP	0.042	0.008
*p*MLS-GFP	0.061	0.01
*p*CgVEGF-HA-IRES-GFP	0.071	0.009
Plasmid Control	0.161	0.008
SuperFect Control	0.017	0.007

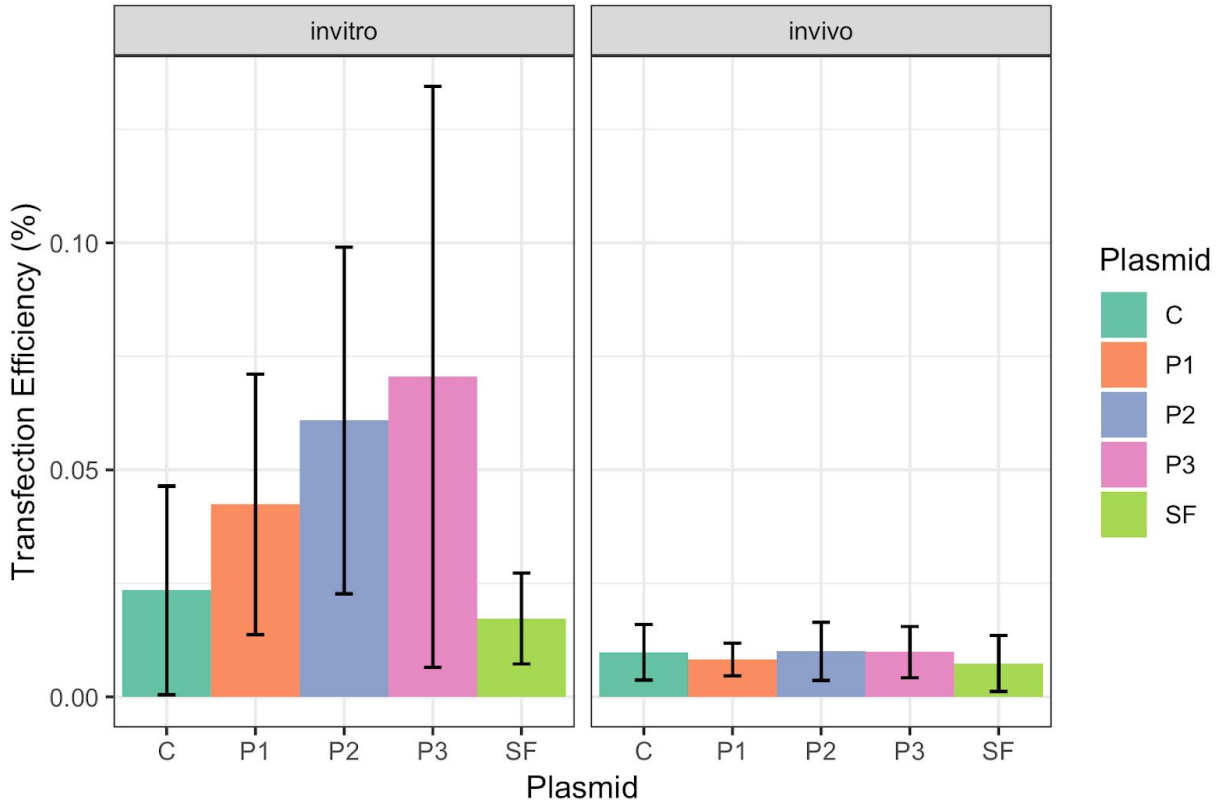

Figure 8. Transfection efficiency of each plasmid treatment compared to control groups using *in vitro* and *in vivo* methods. Where, P1 = *p*max-GFP, P2 = *p*MLS-GFP, P3 = *p*CgVEGF-HA-IRES-GFP, C = transfection serum control, PC = plasmid control, SF = SuperFect control. Data was non-parametric with low sample sizes, and thus, Wilcoxon tests were run between control groups and plasmid groups and no statistical significance was seen with a p-value of 0.47 for both methods.

Median polish non-parametric data analysis of transfection efficiencies showed the two categorical variables that were causing the greatest effects on the total median were the transfection serum control and SuperFect control *in vivo* samples (Figure 9). Meaning, the two

control groups were raising the median transfection efficiency, according to the median polish analysis. However, the largest transfection efficiency effects from plasmid vectors were seen in *p*MLS-GFP and *p*CgVEGF-HA-IRES-GFP *in vitro*. This statistical analysis yields inconclusive evidence given the largest transfection efficiency effects on the median were seen in the control groups. However, when looking at the plasmids, it demonstrated that the *p*MLS-GFP and *p*CgVEGF-HA-IRES-GFP *in vitro* samples showed higher median efficiencies than the *p*max-GFP samples.

When looking at fluorescence over time points of the experiment, we see some statistical significance. The efficiency of transfection seems to increase at each timepoint in most of the plasmid samples (Figure 10). This suggests that more cells express plasmids at 8 days post transfection than 24 hours post transfection with a significant p-value of 0.002 (Wilcoxon non-parametric test). The 3rd experiment was left out of this analysis as the means were so much higher than other experiments and the 8 day time point was inconclusive.

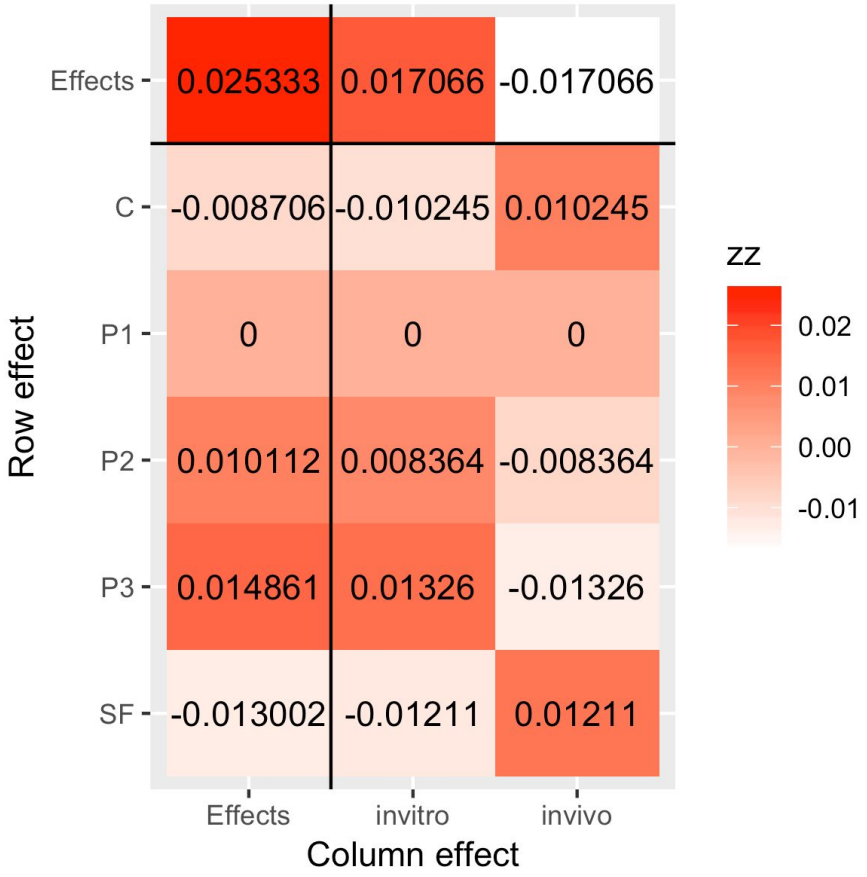

Figure 9. Median polish analysis of non-parametric data. Shows the residual effects of each variable on the mean. ZZ heat map shows the variables with most positive effect in the deeper red colors and most negative effect in white. Where, P1 = *p*max-GFP, P2 = *p*MLS-GFP, P3 = *p*CgVEGF-HA-IRES-GFP, C = transfection serum control, PC = plasmid control, SF = SuperFect control. This shows that the greatest effects were seen in *p*CgVEGF-HA-IRES-GFP *in vitro* and the SuperFect and control *in vivo*. This shows inconclusive effects from the variation in the transfection efficiency due to categorical variables of the flow cytometry data.

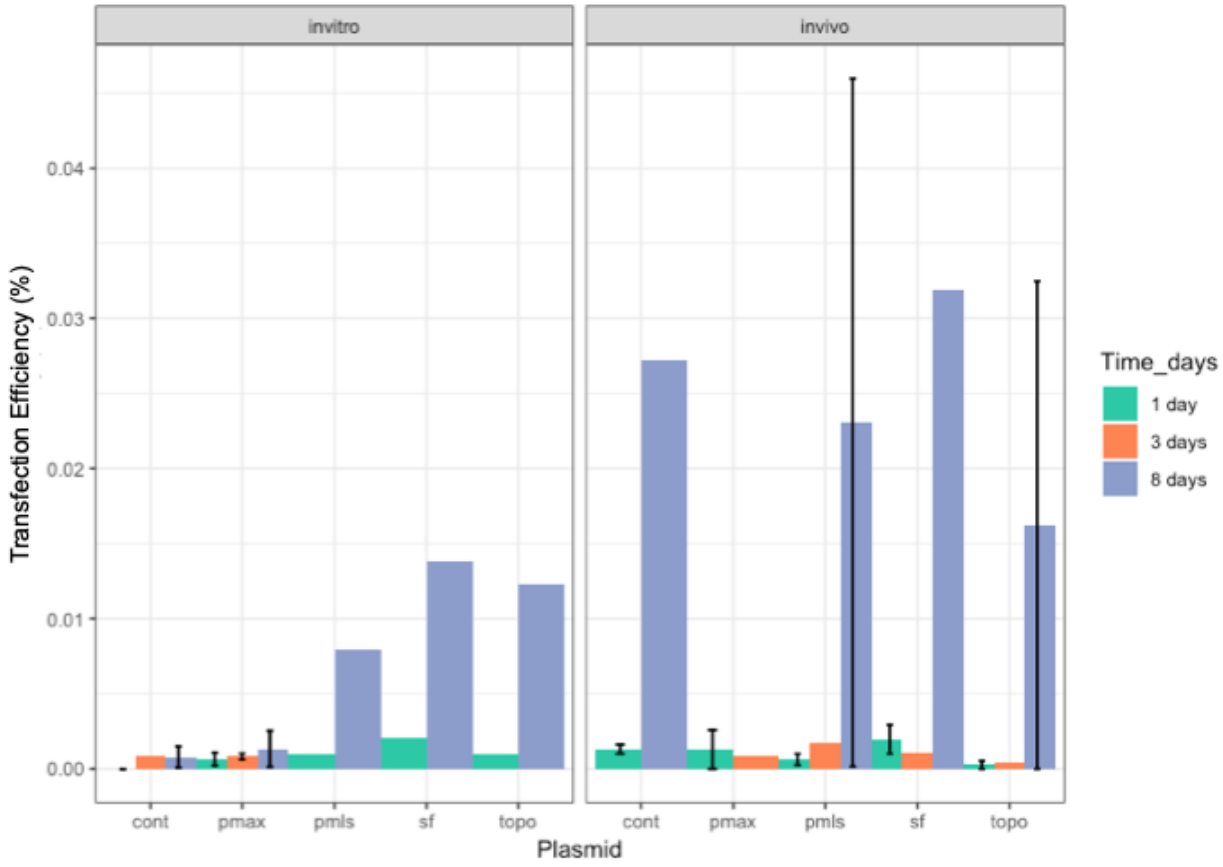

Figure 10. Transfection efficiency of fluorescent plasmid samples over three time points of 1 day, 3 days and 8 days post transfection. The last experiment was not included as transfection efficiency means were higher at all time points and threw off the trend. The 8 day time point was statistically significant from other time points with a p-value of $p < 0.002$ (Wilcoxon non-parametric test).

4.2 Electroporation Results

There was a large number of damaged hemocyte cells seen in the transfected cells (Figure 4. C.). This might suggest cell death, although viability stains were not used . The electroporation method showed very low efficiencies (Table 2, Figure 11). The electroporation means of

transfection efficiency were lower than those of the other two methods and none of the plasmids were significantly different from controls with a p-value of p=0.64 (Wilcoxon non-parametric test) and an n = 2. The total events counted with the flow cytometer in electroporation samples were a full order of magnitude greater than those in other method samples. Moreover, the number of fluorescent cells in the electroporation method were two orders of magnitude lower than other methods. Further data would be needed for concrete statistical results, but due to the large amount of cell damage seen in the confocal microscope, further experiments were halted.

Table 2. Transfection efficiency means (#fluorescent cells/sample) quantified with the flow cytometer with samples from the electroporation method, where none are statistically significant with a p-value of 0.64 and n=2 (Wilcoxon, non-parametric test).

	Transfection Efficiency
Control	3.722905e-05
*p*max-GFP	5.295217e-05
*p*MLS-GFP	1.128863e-04
*p*CgVEGF-HA-IRES-GFP	4.051967e-05

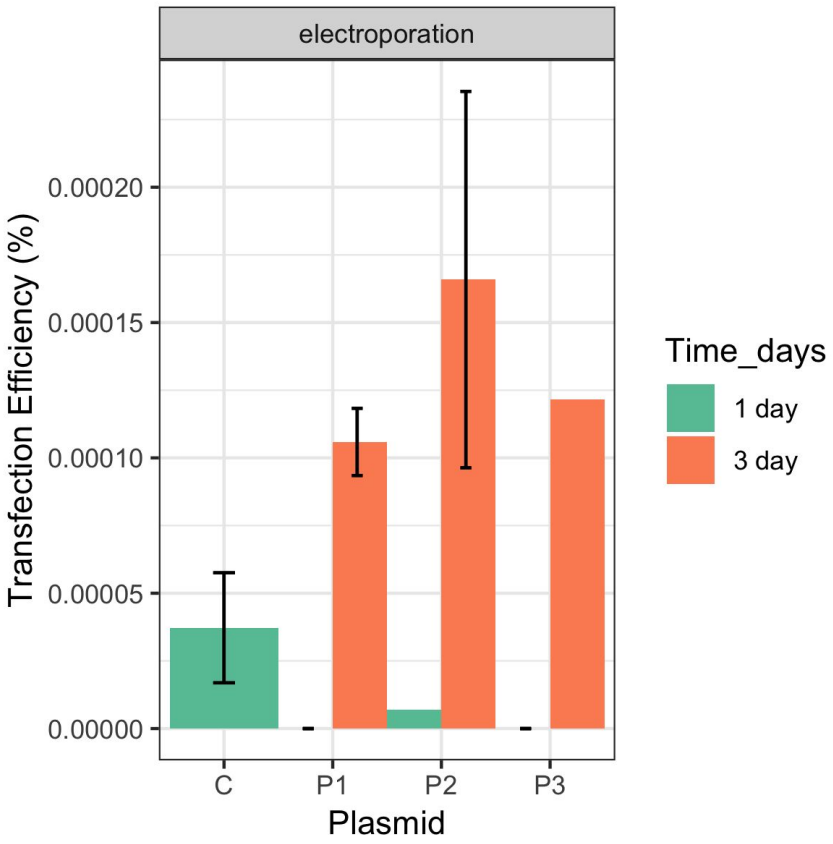

Figure 11. Electroporation transfection efficiencies where mean efficiencies were calculated by total cells divided by fluorescent cells. No statistical significance was found between treatment groups as there was a wide amount of variation in the number of fluorescent cells in each sample with a p-value of p = 0.64 (Wilcoxon non-parametric test).

4.3 Final Experiment Results

The last experiment run had more accurate gates in the flow cytometer and therefore had the most relevant data. The last experiment showed results where the efficiency *in vitro* is 0.07% in *p*max-GFP and 0.13% in *p*CgVEGF-HA-IRES-GFP (Figure 12 A). The *in vivo* results had efficiencies of 0.01% in *p*max-GFP and 0.01% in *p*CgVEGF-HA-IRES-GFP (Figure 12 B).

Neither one had statistically different p-values due to high amounts of variation in each sample. However, this was the highest significance of any experiment done in this project.

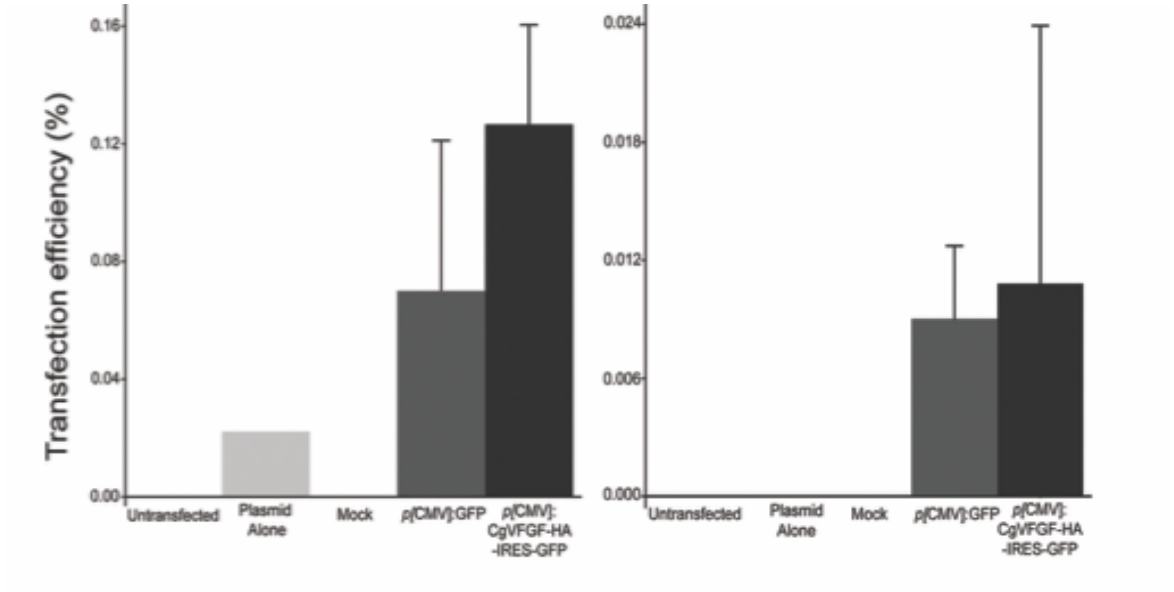

(A) **(B)**

Figure 12. Transfection experiment 4 where the baseline fluorescent efficiency was set as zero and the other efficiencies were corrected. **(A.)** *In vitro* transfection method where plasmid transfection efficiency is higher than the baseline with a p-value of 0.422 and no statistical significance. **(B.)** *In vivo* transfection method where plasmid transfection efficiency is higher than the baseline with a p-value of $p < 0.842$ and no statistical significance (Wilcoxon non-parametric test).

Chapter 5: Discussion

5.1 In Vivo and In Vitro

This study was the first to express plasmid genes *in vitro* in *C. virginica* hemocytes using chemical dendrimers. This method still requires further research in order to optimize it, but it is a starting point in order to move bivalve genetic research forward. While CRISPR-Cas9 is widely available, we need to know more about oyster genes in order to use it efficiently. This is a replicable method that will allow researchers to begin to annotate the oyster genome without the use of expensive equipment, thus saving labs money.

Since cells were seen to be fluorescent as soon as 24 hours after transfection, this suggests that cells were able to uptake the plasmid and express the genes quickly. Other studies found fluorescent hemocytes 4 days post transfection. This demonstrates that our method showed positive results sooner than previous studies, and thus, is more effective for future studies in annotating the genome.

IFA analysis confirms that genes from our plasmids were being expressed in hemocyte cells. Other studies found confirmation of gene expression using IFA of hemocyte cells in *Mytilus edulis*, thus allowing us to conclude that these are positive results (Noël et al., 1996; Pipe, 1990). However, we are the first study to use IFA to confirm transgene translation in oyster cells. The other plasmid vector *p*MLS-GFP did not receive IFA analysis confirmation due to lack of funds and time, but further studies should be done to confirm the expression of the other plasmid's genes. However, we can assume that cells transfected with different plasmids containing GFP genes, such as *p*MLS-GFP, exhibiting similar green fluorescence intensities under the confocal microscope and flow cytometer, are also expressing plasmid genes.

The confocal images show green fluorescent hemocyte cells and non fluorescent hemocyte cells, suggesting that transfection was successful, but not 100% effective. The number

of fluorescent cells per sample varied from oyster to oyster from as low as 0.007% to as high as 0.016%. This was expected as other studies using SuperFect as a chemical transfection agent reported less than 5% transfection efficiency in hemocytes *in vivo* (Buchannan et al., 1999). However, higher transfection efficiencies would be needed to facilitate the annotation of the oyster genome, and this method should be optimized in future studies.

The flow cytometer had gates to ensure the fluorescent cells being counted were only expressing GFP and not chlorophyll pigments. In addition, we set up gates to account for baseline autofluorescence in the hemocytes. That being said, we found that there were still many control cells that made it into our fluorescent gates. Other studies have also reported large amounts of autofluorescence in the hemocytes (Buchannan et al., 1999). However, with each subsequent experiment, the gates became more precise and there were fewer fluorescent control hemocyte cells that were counted. Further research is needed to optimize the counting of fluorescent cells, but our last experiment showed that there were more differences between the efficiencies of controls and fluorescent plasmids than other previous experiments. In order to quantify the number of fluorescent cells, we will have to find a way to set a more accurate background fluorescence threshold that accounts for the significant amounts of autofluorescent variation seen in hemocytes.

While our flow cytometry results were not statistically significant and our efficiencies were low, this was seen in other previous experiments that reported an average of less than 1% fluorescent hemocyte cells in *in vivo* samples (Buchannan et al., 1999). That being said, we were able to find some slight differences that may help us optimize the method in the future. Overall, there may be higher efficiencies in transfection experiments one week post transfection. The

higher transfection efficiencies over each time time point are congruent with results from other studies (Buchannan et al., 1999). However, it is important to note that variability in the number of fluorescent cells also increased with time. Moreover, oyster serum was combined, which may cause issues for isotonic solutions, and may increase hemocyte autofluorescence. Further experiments should be done to see if this is true.

5.2 Electroporation

Large amounts of cell damage was seen in electroporated hemocyte cells under the confocal microscope and fewer cells were seen fluorescing in those samples. As electroporation is associated with decreased embryo cell survival, these results were expected (Lu et al. 1996; Buchannan et al., 1999). The electroporation method gave an order of magnitude higher of event counts and two orders of magnitude lower of fluorescent cells than other *in vitro* and *in vivo* methods. This may suggest that there was higher amounts of cell damage from electroporation methods than methods using the chemical dendrimer SuperFect.

The high amounts of cell damage seen in the electroporated hemocytes suggests that SuperFect transfection dendrimers are a better transfection method, as it is less time consuming, less expensive, and results in lower amounts of cell damage. In fact, SuperFect has a statistically insignificant toxic effect on oyster embryos and hemocytes (Buchannan et al., 1999). In the future, researchers should use the SuperFect method outlined in this paper to annotate the oyster genome.

5.3 Possible reasons for variation

Several issues occurred with differentiating GFP from autofluorescence in hemocytes. Other studies have seen green autofluorescence in hemocyte cells of several mollusks and bivalve species (Johnston & Yoshino, 2001; Vasta et al, 1984; Buchannan et al. 1999). Moreover, it was found that different individual oysters varied in the amount of autofluorescence and success of transfection (Buchannan et al. 1999). This caused issues in differentiating GFP from other green autofluorescence found in hemocytes, however our study set gates that attempted to exclude autofluorescent levels in order to differentiate the fluorescent intensity of autofluorescence versus GFP expression.

Other studies have found autofluorescence in several cell types in the Eastern oyster such as hepatopancreas cells, mantle cells and sperm cells (Ringwood et al., 2009; Richards et al., 2018; Vignier et al., 2017). In addition, it was found that some algae that are ingested by the oysters exhibit photosynthetic autofluorescence (Epinosa et al., 2018). These algae cells could have been withdrawn from an *in vivo* oyster if the adductor muscle was missed during hemolymph withdrawal and cells were withdrawn from the pallial cavity instead. This is likely why we see some cells faintly fluorescing green under the confocal microscope and why some cells expressed chlorophyll a in the flow cytometer. This may be the reason we are not getting statistically significant data from the flow cytometer. Future studies may attempt to treat samples with antibiotics in order to control for non-hemocyte cells without transgene expression.

The hemolymph withdrawal techniques are an established method (Buchannan et al., 1999; Larson et al., 1989), but do require the researcher to be attentive about where the hemolymph is withdrawn. The oyster muscle feels firm and puts up some resistance when it is stuck with the needle. However, if the needle misses the muscle, many different cell types are

withdrawn from the mantle, pallial cavity, or digestive gland of the oyster. In bad draws, there were some cells expressing chlorophyll pigments. This is presumably phytoplankton or cyanobacteria that are the primary food of the oyster and can be found in the pallial cavity or digestive system of the oyster (Epinosa et al., 2018). As chlorophyll pigments were seen in the flow cytometer results, we can assume that bad hemolymph draws may have been behind some of the variation seen in cell counts.

To combat this autofluorescence, we used gates to ensure that the green fluorescence we saw was more than the faint green autofluorescent intensity. We used the amount of autofluorescent intensity seen in control hemocyte samples as the baseline and set gates at those points. The fluorescent cells that were counted were actually fluorescing more intensely than the autofluorescence seen in other control cells. Thus, any cells that had higher green fluorescent intensities were considered positive for GFP.

The timing between notching the oysters and transfection varied due to scheduling and as a result oysters recovered for up to one week or as little as 24 hours post notching before transfections were performed. We found that experiments performed only 24 hours post notching had higher efficiencies (final experiment) than the experiments performed one week post notching (all other experiments). It has been found that hemocytes, specifically granulocytes, take part in carrying calcium through the organism to regenerate the shell matrix (Mount et al. 2004). This means that hemocytes are likely to be highly stimulated after notching and are more likely to express genes during this time. As a result, further studies should transfect approximately 24 hours post notching in order to increase transfection efficiencies.

5.5 Future Directions

The immediate next steps will be to optimize the method. There are several ways to do this by changing some of the methodological variables. For example, we could change the ratio of SuperFect to plasmid as done in Buchannan 1999, which could increase transfection efficiencies. For *in vitro* studies, increasing the density of hemocytes in wells may lead to higher transfection efficiencies, as there were lower transfection efficiencies in the more diluted *in vivo* transfections. In addition the use of homologous promoters, or promoters found in Eastern oyster DNA, may lead to the increased expression of transgenes.

Future studies should run viability tests to see if SuperFect is toxic to oyster hemocytes and at what time points and concentrations. Previous studies found SuperFect to be toxic to oyster valve cells, but not embryos (Buchannan et al., 1999) and understanding toxicity effects on hemocytes would be important for the continued use of this method. This may give some needed guidance to what the next optimization steps will be.

Notching the posterior dorsal side of oyster shells did not cause death in any live oysters, meaning it is a viable method for hemolymph extraction (Yang et al. 2013), however timing before transfection may influence the hemocytes as shell regeneration is mediated by granulocytes (Mount et al. 2004). In addition, future studies should look into the proper temperature at which to incubate the oysters and hemocytes post transfection as higher temperatures increase metabolic rate and may increase the rate of transfection and gene expression (Welsh et al. 2015).

Once the method is optimized, researchers can begin to examine the genome. There are over 32,000 predicted genes in the Eastern oyster genome and many of them are novel

(Gomez-Chiarri et al., 2015). By using the method we developed, we can begin to insert predicted genes, promoters and enhancers into the multiple cloning site of any of our tested plasmids. This will allow us to see the gene, promoter or enhancer expression tagged with GFP fluorescence and begin to understand the function of these novel genes. This will allow us to annotate each part of the genome and better understand the importance of the function of different genes.

As outlined in my introduction, once the genome is examined, it can be used to continue research on the many medical, economic, and conservation applications, as well as cell line development. A well annotated genome can give better scientific information to aquaculturists, when artificially selecting for disease resistant traits to breed (Yang et al. 2013). In addition, further knowledge of gene function can be used to further medical research in bone regeneration, innate immunity, microbiomes, and cancer (Fernández Robledo et al. 2018). Further genetic discovery could also lead to the understanding of which genes allow oysters to live in more nutrient rich areas, thereby educating conservationists on which traits to select for when rehabilitating oyster reefs (Smyth, 2013; Bricker et al. 2018; Gàrate et al. 2019). A well annotated oyster genome may even shed light on the research behind developing bivalve cell lines. This method is the first step to many possible ground breaking applications.

Chapter 6: *Mercenaria mercenaria* Transfection

6.1 Introduction

While oysters are an incredibly under studied bivalve, genetically speaking, clams are in a similar position. A cell line has not been developed and many genes have not yet been

annotated (Yoshino et al., 2001; Buolo et al., 1996). By taking our established transfection method and using it successfully in other bivalves, we can broaden the impact of this research. It could theoretically work in any bivalve with a few optimization modifications, and this would allow scientists to further examine the genomes of all species in this class.

Quahog clam, or *Mercenaria mercenaria,* aquaculture is a large economic industry on the East coast of the United States. *M. mercenaria* is affected by the protozoan parasite called QPX, which is decreasing their population sizes (Bassam & Allum, 2018; Hartman et al., 2018; Wang et al 2016). The genetic backgrounds of each clam either drives the clam toward immunity or death by the parasite (Bassam & Allum, 2018). Moreover, several bivalve species have been associated with microbiomes containing denitrifying bacteria (Welsh, 2015). Further genetic study of these interactions is needed to understand how to protect the quahog aquaculture industry from this parasite and increase denitrification to ameliorate nitrogen pollution.

Previous studies have transfected surfclam embryos using electroporation methods, but saw only 3-5% embryonic survival post electroporation (Lu et al., 1996). We believe that the SuperFect dendrimers will cause less cell damage and will be a viable method for transfection clam hemocytes, given that this method works in oyster hemocytes.

6.2 Methods

Quahog clams were transfected using the *in vivo* and *in vitro* methods stated above in chapters two and three. The same incubation styles were used in buckets and 12-well plates in a 12-16˚C incubator. The same data analysis methods were used with flow cytometry, and confocal microscopy. The same gates were used in flow cytometry and confocal microscopy in

order to avoid potential autofluorescence. However, the GFP and HA IFA was not done due to time and financial constraints.

6.3 Results and Discussion

M. mercenaria hemocyte cells showed fluorescence under the confocal microscope 24 hours post transfection. The mean transfection efficiency from the flow cytometry showed lower efficiencies than those seen in *C. virginica* (Table 3). The efficiencies were not statistically significant from controls and had wide amounts of variation (Figure 13). *In vitro* mean transfection efficiencies were much lower than *in vivo* mean transfection efficiencies. The *M. mercenaria* efficiencies did not seem to increase at each time point in contrast with *C. virginica* mean efficiencies.

This experiment shows that this method can be used in other bivalve species. However, there was a large amount of variation in the control transfection efficiencies, which may be due to gating issues with the flow cytometer. Further research should be done on proper flow cytometry and confocal microscope gating in order to reduce autofluorescence. Once this method is optimized for each species, this preliminary experiment shows that this method can be used to annotate the genomes of several different bivalve species.

Table 3. *M. mercenaria* transfection efficiencies (#fluorescent cells/sample) by plasmid measured by flow cytometry. No transfection efficiencies were statistically significant and there was a large amount of variation in each sample with an n = 3.

	In vitro	*In vivo*

Control	0.002665917	0.010895530
*p*max-GFP	0.000973086	0.002523726
*p*MLS-SV40-GFP	0.001673409	0.003245175
*p*CgVEGF-HA-IRES-GFP	0.001191304	0.003592762
SuperFect Control	0.000361136	0.006620356

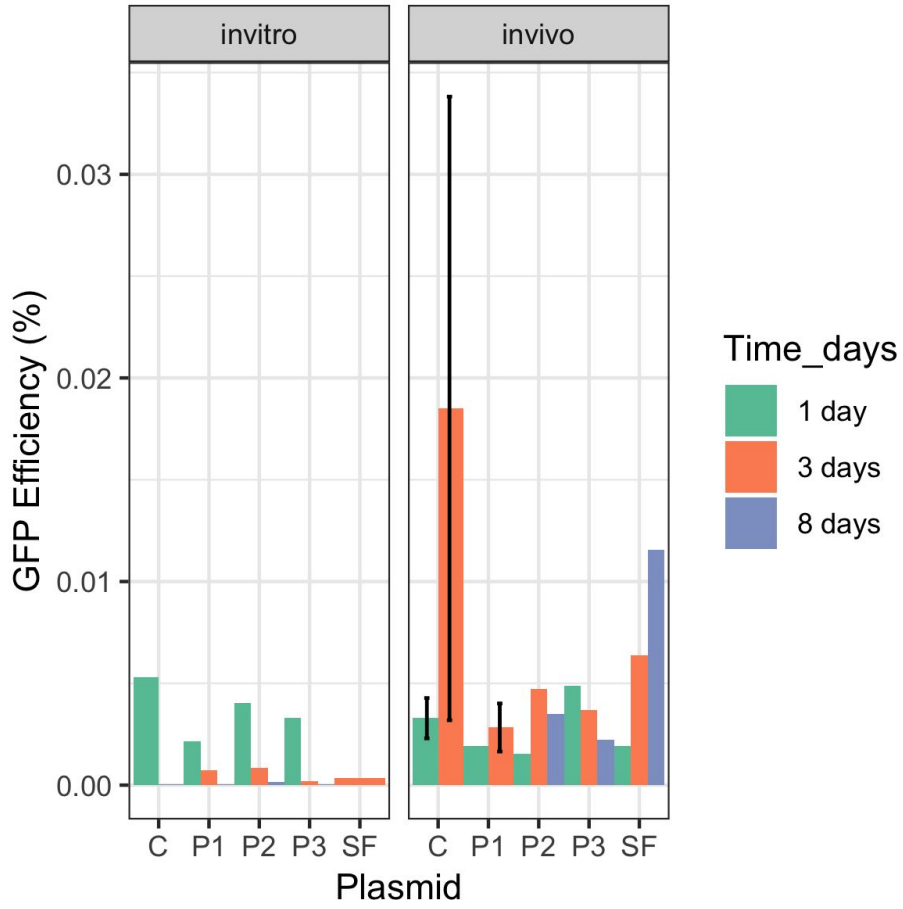

Figure 13. *M. mercenaria* mean transfection efficiencies at three time points, with three different plasmids. Where, P1 = *p*max-GFP, P2 = *p*MLS-GFP, P3 = *p*CgVEGF-HA-IRES-GFP, C = control, PC = plasmid control, SF = SuperFect control. No statistical significance with n = 3.

Chapter 7: Cell Line Development Experiments

7.1 Introduction

While the cell line of oysters has not been developed yet (Yoshino et al., 2001; Boulo et al. 1996), there are several genes of interest that may lead to cells living and dividing in culture. The small T antigen gene comes from simian virus 40 and causes rapid cell growth by accelerating G1 and S phases of the cell growth cycle (Uniprot.org). The hTert gene codes for a ribonucleoprotein enzyme, from human cancer cells, that elongates the telomeres of chromosomes during DNA replication and allows the cell to live longer (Uniprot.org). Through our transfection method we can introduce these plasmids into oyster blood cells and embryos. Given the circulation system of the oyster, these plasmid genes may travel to other tissues of the oysters (Buchannan et al. 1999). By using these "immortalization" genes in plasmids, we hope to increase the lifespan and growth of cells in culture, and potentially get cells in primary cultures to divide.

7.2 Explant Transfection

7.2.1 Methods

Six oysters were transfected *in vivo* with *p*cDNA-3HA-hTert (Add Gene) or *p*Babe-GFP-Small T Antigen (Add Gene). The six oysters transfected were dissected and

explants were cultured to see if transfected tissue cells would divide in culture. Explants from adductor muscle, edge mantle, soft mantle, heart, gills and palps were taken from each oyster and dried on a paper towel for about 30 seconds (Figure 14). All dissection tools were sterilized with 70% Ethanol and burned before and after each oyster dissection. Each explant was treated with either antibiotics or ethanol for 10 seconds then placed in wells containing growth medium (Boulo et al., 1996). The antibiotic treatment was made of Penicillin, Streptomycin, Kanamycin, Neomycin, Nystatin, Erythromycin, Gentamycin, Polymixin-B, Tetracycline, Vancomycin (Appendix D) (Polne-Fuller, 1991). The medium was made of Leibovitz 2X mOsm with a pH of 7.5 and had an added 10% FBS (Gibco/BRL) (Boulo et al., 1996). Each plate of wells was incubated at 12 ˚C while monitored for cell proliferation and division. Wells were observed using an inverted microscope.

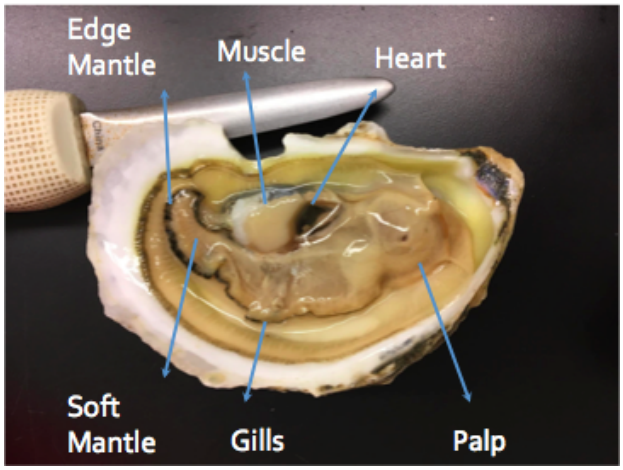

(A.)

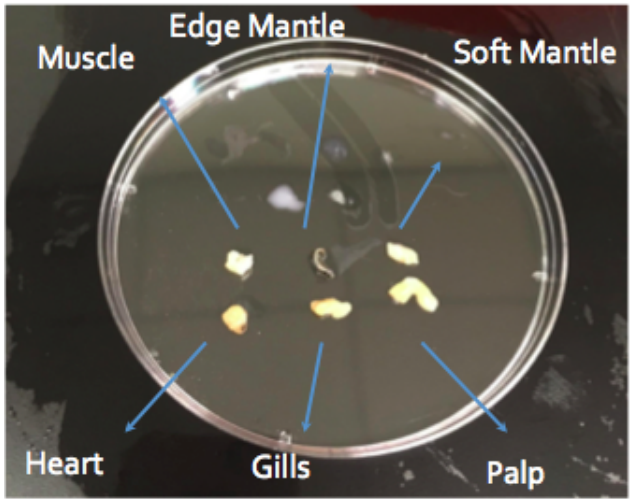

(B.)

Figure 14. (A.) Eastern oyster dissection diagram of locations of different tissues where explants were removed. **(B.)** The explants from each tissue of the dissected oyster before transfection.

7.2.2 Results

Cells were looked at under the inverted microscope at 10x and 400x, every few days (Figure 15). The cells exhibited some adherence to the well. Using epifluorescence, some cells exhibited green fluorescence showing that transfection was likely successful. There was a great deal of contamination in some wells, especially those treated with ethanol, which led to a high turbidity and made it difficult to examine cells. No cell division was seen after one week of incubation, but there were some signs that the cells were accepting the medium, or exhibiting their ability to stay alive in the medium. Cells were seen with cilia movement and one heart explant was seen beating in the medium. Well contamination continually increased and cell division did not occur. After one month of incubation, the experiment was halted due to excessive contamination.

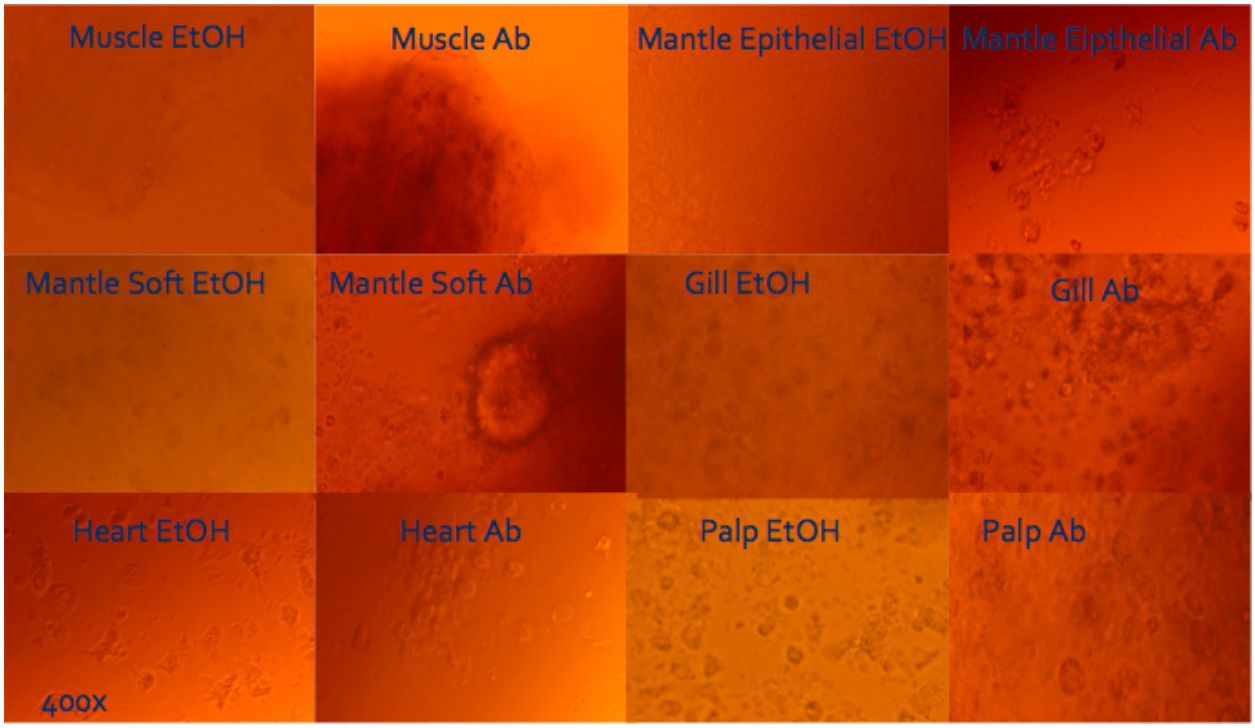

Figure 15. Transfected explants under the epifluorescent microscope at 400x. Each explant was put in the same Leibovitz 2X mOsm with a pH of 7.5 and had an added 10% FBS (Gibco/BRL) media with either an ethanol treatment (EtOH) or antibiotic cocktail treatment (Ab) to reduce contamination.

7.2.3 Discussion

The cells did not proliferate or divide, however we can tell that the cells accepted, and can survive in, the growth medium. The continuation of muscle contractions in the heart explant and the moving cilia on cells, suggest that the cells are still alive and functioning. Beyond that, few conclusions can be made without further data and information. After several weeks of incubation the contamination forced the experiment to be terminated. In the future, slight

changes to media and incubation techniques may yield longer incubation times and possible cell proliferation.

7.3 Embryonic Transfection

7.3.1 Methods

Approximately 1L of oyster embryos were procured from Mook Sea Farms (Bristol, ME) at 5pm after spawning earlier that day. Embryos were transfected with *p*cDNA-3HA-hTert (Add Gene), *p*Babe-GFP-SmallTAntigen (Add Gene) that night before embryos began to clump and divide.

Fifty mL of embryos were pipetted into 12 separate 50 mL Falcon Tubes. Each tube was centrifuged at 200 g for 2 minutes at 18˚C. The supernatant was removed and 50 additional mL of embryos were pipetted into the Falcon Tubes. This was repeated approximately three times until a visible pellet formed in the Falcon Tubes. 40 mL of supernatant was removed from the tubes leaving 10mL of supernatant and the pellet was resuspended in those 10mL. The volumes of two tubes were added together to total 20 mL of embryos in six Falcon Tubes. These tubes were centrifuged again at 200 g for 2 minutes at 18˚C. 19 mL of supernatant were removed and the pellet was resuspended in the 1 mL leftover volume. The volume from each tube was transferred into a 12-well incubation plate.

The 5 µg of pDNA was resuspended in 33µL of Alsever's. 67 µL of SuperFect was added to the plasmid solution for a total volume of 100 mL. The solution was added to each 12-well plate and was incubated at 11-18˚C for two hours. The embryos were then dissociated after the two hour incubation.

250µL were taken from each well of transfected embryos and added to a 1.5 mL Eppendorf Tube. The Eppendorf tubes were centrifuged at 100g for 2 minutes. The supernatant was removed and the pellet was resuspended in 62.5 µL of calcium free seawater (CFSW). The tube was centrifuged at 100g for 2 minutes. The supernatant was removed and the pellet was resuspended in 62.5µL of calcium - magnesium free seawater (CMFSW). The tube was centrifuged at 100g for 2 minutes. 50 µL of supernatant was removed and the pellet was resuspended in 62.5µL of CMFSW. The 12.5µL embryo suspension was aspirated and dispensed. 1mL of the L15 Media and 100µL of the antibiotic cocktail was added to each tube. The pellets were resuspended and the solution was transferred into 12-well plates and incubated at 11-18˚C. Cells were analyzed and imaged under an epifluorescence microscope every few days post transfection for approximately one month. L15 media was changed 17 days post transfection.

7.3.2 Results and Discussion

Using the epifluorescent microscope, green fluorescence was seen 24 hours post transfection in transfected cells that were identified to be embryos (Figure 15), although no IFA analysis was used to confirm expression of our specific genes. Fluorescence was seen in cells transfected with plasmids containing GFP genes, but not in controls or plasmids not containing fluorescence, pcDNA-3HA-hTert, Embryo Control and SuperFect Control (Figure 16). Clumps of embryos did not form in wells, suggesting that dissociation was successful. The cells adhered to the bottom of the wells for the first two days after transfection and then detached from the bottom of the wells.

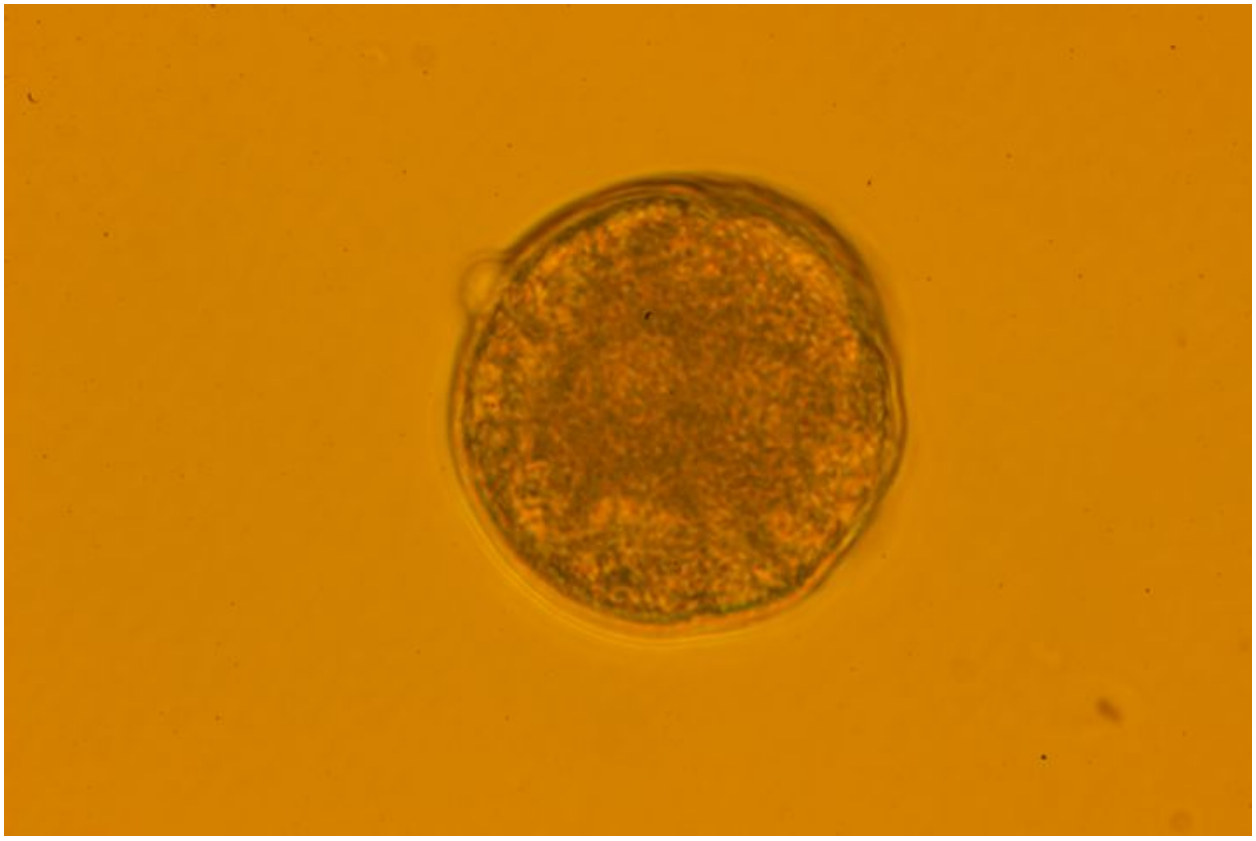

Figure 15. Blastula stage Eastern oyster embryo found in 12-well plate post transfection. Indicates that embryo cells continued to live in incubation media and remained dissociated after transfection.

Contamination was found in the wells after four days and continued to worsen as the experiment progressed. Crystals began to form in the media even after the media was changed at 10 days post transfection. Fluorescence was seen in crystals that formed in the media (Figure 16) and fluorescence was seen in untransfected embryo control, pcDNA-3HA-hTert, and SuperFect control starting 16 days post transfection and was widespread at 23 days post transfection. Cell proliferation and division were not seen after 23 days and the experiment was halted due to excessive contamination, wide spread fluorescence in controls, and media crystallization.

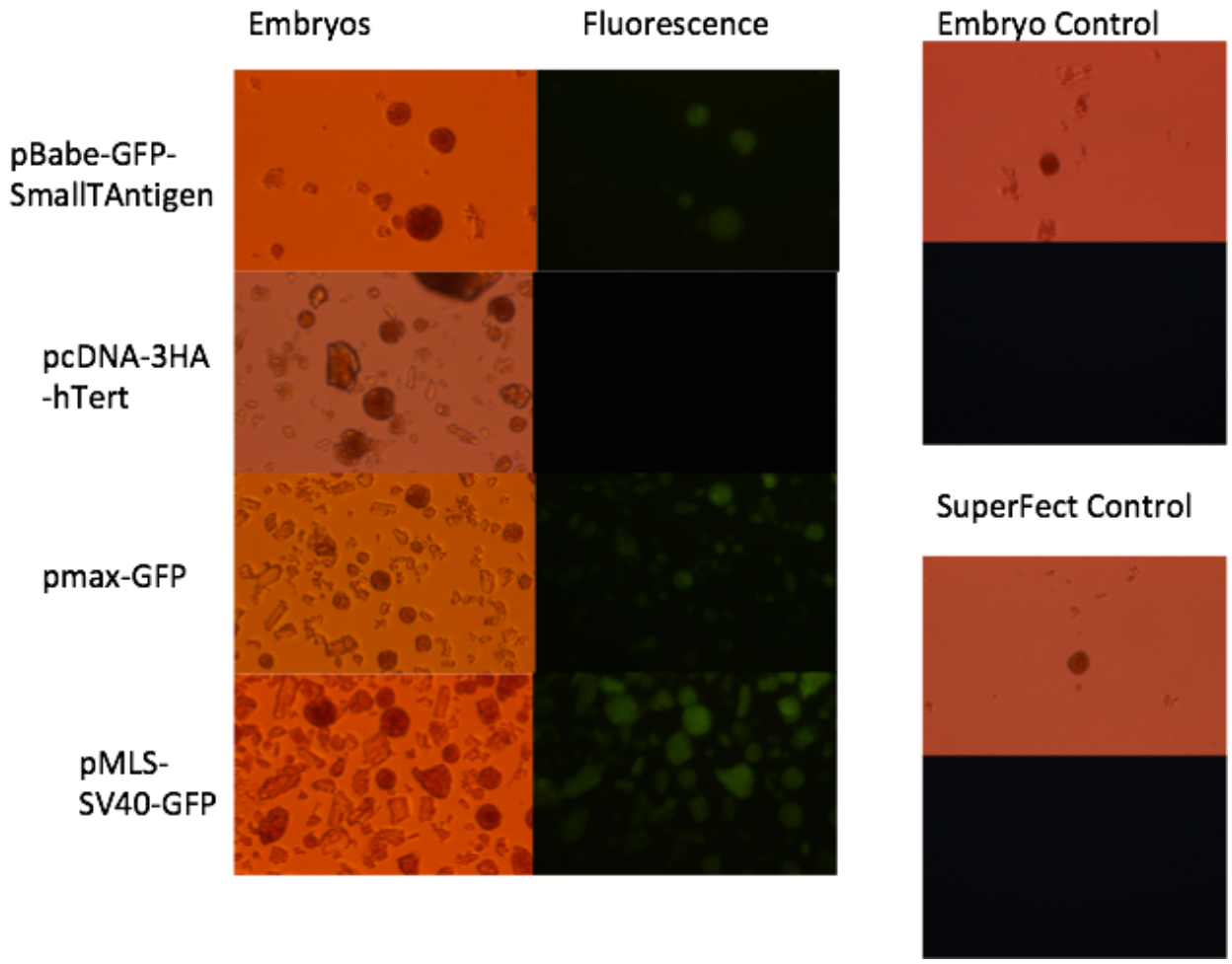

Figure 16. Eastern oyster embryos approximately 10-16 days post transfection at 200x under the epifluorescent microscope. All embryo cells were transfected with SuperFect *in vitro* method and L15 media was changed at 17 days post transfection.

While the embryos were transfected with plasmids coding for "immortalization" genes, such as *p*cDNA-3HA-hTert (Add Gene), and *p*Babe-GFP-SmallTAntigen (Add Gene), no cell proliferation or cell division was seen. As no other lab has been able to see bivalve cell division in culture after one month, this was expected (Buolo et al. 1996). This may have been due to the conditions of the incubation temperature or media used. The embryonic transfection showed

fluorescent embryo cells under the microscope, however no IFA analysis was done to confirm gene expression. As other oyster embryonic studies found between 13 and 33% transfection efficiency (Lu et al. 1996), our embryo fluorescence was expected and was seen in several cells in each plate. The contamination became widespread after four days and as a result other sterilization methods should be employed. Further studies should be done using the transfection method to attempt to develop a bivalve cell line by changing some of the incubation variables we used.

Chapter 8: Homologous Promoter Amplification and PCR

8.1 Introduction

The idea behind this method is to be able to express homologous oyster genes or promoters tagged with GFP so researchers can see where, when, and how long gene expression occurs in the oyster (Cheikh et al., 2017). This will allow scientists to examine the oyster genome more adeptly and accurately. For that reason, one of our supplemental experiments was to express the homologous gene, actin, which is a protein found in the cytoplasm of oyster hemocytes and muscle cells (Cadoret et al., 1999). This will show how the protein functions in the cell when gene expression is activated. Actin is a homologous oyster gene that is highly expressed in hemocyte cells, as the protein forms the cytoskeleton that is used in phagocytosis (Cadoret et al., 1999). While the promoter region of this gene is not known, the protein coding sequence has been identified. By amplifying the expected promoter region of this homologous gene, and inserting it into a plasmid vector, it can be transfected. Post transfection we will likely see the fluorescence of the GFP promoter at actin's normal rate in hemocyte cells. Perfecting this

method will allow us to see how any gene functions in the oyster, and help to examine the oyster genome as well as that of other bivalves.

8.2 Methods

Actin primers were designed with the idea of locating the promoter region of the gene, which is unknown. Four primer pairs were chosen, amplifying either 1000bp in the 5' region of the gene, 100bp in the 5' region of the gene, 1000bp in the 5' region of the gene with 10 amino acids of the protein sequence, or 100bp in the 5' region of the gene with 10 amino acids of the protein sequence.

Genomic DNA was extracted from oyster gill, hemocyte, rectum, heart, mantle, and muscle. Muscle DNA was used to amplify actin primers. 4µL of genomic DNA, 0.5µL actin forward primer, 0.5µL backwards primer, 12.5µL EconoTaq Polymerase, and 7.5µL deionized water were combined for a total of 25µL. PCR was run in the BioRad C1000 Touch Thermocycler on each of the four primer pairs. The PCR run was at 95˚C for 3 minutes, 95˚C for 30 seconds, 55.6˚C for 30 seconds and 72˚C for 5 minutes and this cycle was repeated 34 times. Then the PCR ran at 72˚C for 5 minutes and went to 4˚C indefinitely to preserve the DNA. A 1.4% electrophoresis gel was run with the PCR DNA to check sizes. The gel was run at 70 V with 8 µL of Midori Green. Each well contained 10µL of DNA, and 6µL of the NEB 1000kb ladder was used with 5µL of DNA loading dye (NEB).

A gradient PCR was run with 8, 25µL PCR tubes for each of four primer pairs totaling 32 PCR tubes. Each tube contained 4µL of genomic DNA, 0.5µL actin forward primer, 0.5µL backwards primer, 12.5µL EconoTaq Polymerase, and 7.5µL deionized water which was

combined for a total of 25µL. PCR was run in the BioRad C1000 Touch Thermocycler on each of the four primer pairs. The PCR run was at 95˚C for 3 minutes, 95˚C for 30 seconds, with a varying annealing temperature for each tube for 30 seconds, and 72˚C for 5 minutes. This cycle was repeated 34 times. The PCR then ran at 72˚C for 5 minutes and went to 4˚C indefinitely to preserve the DNA. This allowed each tube to be run at a different annealing temperature starting at 44.6˚C, increasing to 65˚C sequentially from tube 1-8. A 1.4% electrophoresis gel was run with the PCR DNA to check sizes. The gel was run at 70 V with 8 µL of Midori Green. Each well contained 10µL of DNA and 6µL of the NEB 1000kb ladder was used with 5µL of DNA loading dye (NEB).

Primer pair three, with amplified 1000 bp of the 5' region of the actin exon, was run again on its own since it had bands that seemed to be the right size. 4µL of genomic DNA, 0.5µL actin forward primer, 0.5µL backwards primer, 12.5µL EconoTaq Polymerase, and 7.5µL deionized water were combined for a total of 25µL. PCR was run in the BioRad C1000 Touch Thermocycler on each of the four primer pairs. The PCR run was at 95˚C for 3 minutes, 95˚C for 30 seconds, 55.6˚C for 30 seconds, and 72˚C for 5 minutes, and this cycle was repeated 34 times. Then the PCR ran at 72˚C for 5 minutes and went to 4˚C indefinitely to preserve the DNA. A 1.4% electrophoresis gel was run with the PCR DNA to check sizes. The gel was run at 70 V with 8 µL of Midori Green. Each well contained 10µL of DNA and 6µL of the NEB 1000kb ladder was used with 5µL of DNA loading dye (NEB). Bands of the expected 1000bp were extracted and sent for sequencing. The sequenced bands were then used in a TATA cloning method, using the *p*GEM-T plasmid Easy Vector Systems, and IPTG/X-Gal or blue/white

selection was attempted in order to sequence the amplified actin again. However, this was not successful and this section of the project is still in progress.

8.2.1 Results

The actin primers were designed from four different areas of the actin locus in an attempt to amplify the promoter region of the gene (Figure 17). Primer pairs amplified regions including 100bp 5' of the 5' UTR through to 10 amino acids of the exon, 1000bp 5' of the 5' UTR through to 10 amino acids of the exon, 100bp 5' of the 5' UTR through to first base pair of the 5' UTR, 1000bp 5' of the 5' UTR through to first base pair of the 5' UTR (Figure 17).

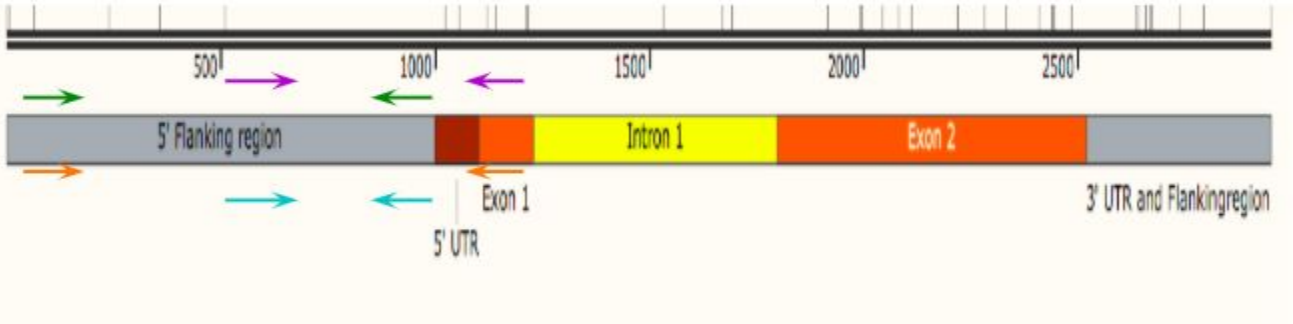

Figure 17. Areas of actin amplified by the primer pairs tested in hopes to amplify the promoter region. The areas amplified were 100bp 5' of the 5' UTR through to 10 amino acids of the exon (Purple), 1000bp 5' of the 5' UTR through to 10 amino acids of the exon (Orange), 100bp 5' of the 5' UTR through to first base pair of the 5' UTR (Blue), 1000bp 5' of the 5' UTR through to first base pair of the 5' UTR (Green). See Appendix C for full plasmid diagram.

When the primers were amplified, the first time, PCR was unsuccessful. The second PCR run was a gradient PCR, in order to find the correct annealing temperature (Figure 18). Primer

pair three, which amplified the 1000bp 5’ of the 5’ UTR to the start of the 5’ UTR coding region, had the correct length band in the electrophoresis gel. The correct sized bands from the gel exhibited the correct sequence of the actin 5’ region. However, when this PCR was TA cloned, the sequence did not match the actin 5’ region. This project is still ongoing and will attempt to find out what went wrong with the TATA cloning.

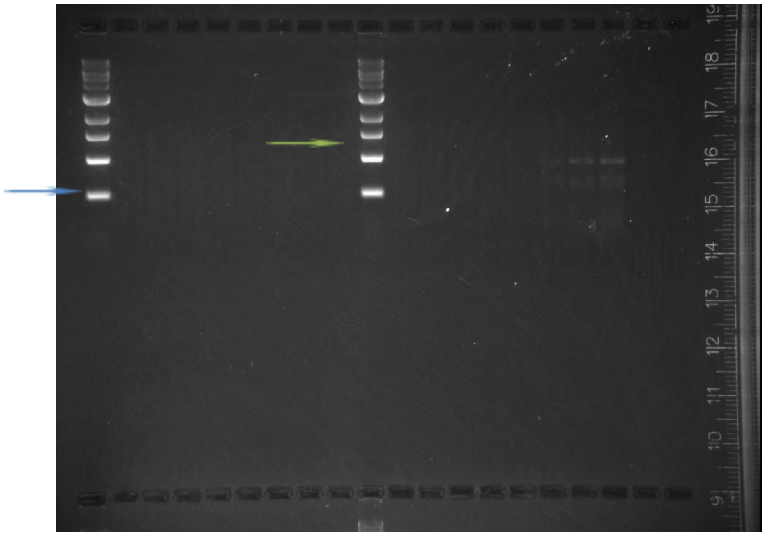

(A) (B)

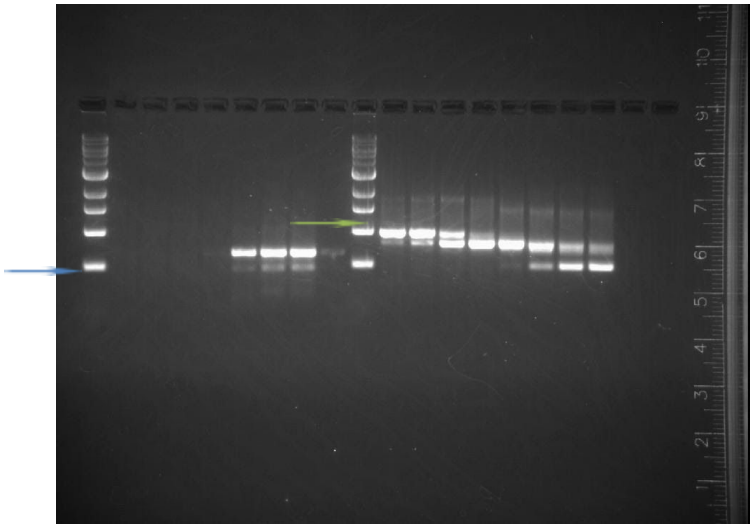

(C) (D)

Figure 18. The gradient PCR electrophoresis gel results, where blue arrows represent either 100bp of expected results and green arrows represent 1000 bp of expected results. (A) Primer pair 1 amplifying the 1000bp 5' of the 5' UTR to 10 amino acids of the exon coding region. (B) Primer pair 2 amplifying the 100bp 5' of the 5' UTR to 10 amino acids of the exon coding region. (C) Primer pair 4 amplifying the 100bp 5' of the 5' UTR to the start of the 5' UTR of coding region. (D) Primer pair 3 amplifying the 1000bp 5' of the 5' UTR to the start of the 5' UTR of coding region.

8.3 Discussion

The actin was amplified in a way that was similar to what was done in Cadoret et al. 1999 in *Crassostrea gigas*, where *C. virginica* primers were used to amplify the *C. gigas* actin with PCR. This process yielded more than one positive clone of the gene. Our first sequencing yielded a positive clone of the actin gene. However, TA cloning did not yield the positive result that was found in Cadoret et. al., 1999 The difference was that Cadoret et al., 1999 used PCR-Script cloning vector and this may be worth trying in further experiments (Cadoret et al., 1999).

The actin amplification hit a roadblock after TATA cloning. This shows that although the actin gene may be highly expressed in Eastern oyster hemocytes, it may be difficult to clone and insert into plasmids. Other homologous genes may be more effective for studying homologous function.

Acknowledgements

A special thanks to José A. Fernández Robledo, Raghavandra Yadavalli, Birdie Waugh, Kosuke Umeda, Kiara S. Reed, David Bishop-Bailey, Dave Angellini, Ron Peck, Bigelow

Laboratory for Ocean Science, NSF Grants #1701480, National Science Foundation Research Experiences for Undergraduates (REU), #1460861 and Colby College Davis Connect fellowship.

References

1. Ansari, S. A., Safak, M., Gallia, G. L., Sawaya, B. E., Amini, S., & Khalili, K. (1999). Interaction of YB-1 with human immunodeficiency virus type 1 tat and TAR RNA modulates viral promoter activity. *Journal of General Virology, 80*(10), 2629-2638. doi:10.1099/0022-1317-80-10-2629

2. Arfken, A., Song, B., Bowman, J. S., Piehelr, M. (2017). Denitrificaiton potential of the eastern oyster microbiome using a 16S rRNA gene based metabolic inference approach. *PLoS ONE* 12(9).

3. Bachere, E., D. Chagot, & H. Grizel. (1988). Cell separation by centrifugal elutriation. In: Disease Processes in Marine Bivalve Molluscs, Vol. 18. W. S. Fisher (ed.). American Fisheries Society, Betheda, MD. pp. 169-177.

4. Bassim, S., & Allam, B. (2018). SNP hot-spots in the clam parasite QPX. *BMC Genomics, 19*(1).

5. Beck, M. W., Brumbaugh, R. D., Airoldi, L., Carranza, A., Coen, L. D., Crawford, C., Defeo, O., Edgar, G. J., Hancock, B., Kay, M. C., Lenihan, H. S., Luckenbach, M. W., Toropova, C. L., Zhang, G., Guo, X. (2011). Oyster Reefs at Risk and Recommendations for Conservation, Restoration, and Management. *BioScience*, *61*(2), 107–116. https://doi.org/10.1525/bio.2011.61.2.5

6. Bernard, I., de Kermoysan, G., & Pouvreau, S. (2011). Effect of phytoplankton and temperature on the reproduction of the Pacific oyster Crassostrea gigas: Investigation through DEB theory. *Journal of Sea Research*, *66*(4), 349–360. https://doi.org/10.1016/j.seares.2011.07.009

7. Boulo, V., Cadoret, J. P., Le Marrec, F., Dorange, G., & Mialhe, E. (1996). Transient expression of luciferase reporter gene after lipofection in oyster (Crassostrea gigas) primary cell cultures. *Molecular Marine Biology and Biotechnology*, *5*(3), 167–174.

8. Bricker, S. B., Ferreira, J. G., Zhu, C., Rose, J. M., Galimany, E., Wikfors, G., Saurel, C., Miller, R. L., Wands, J., Trowbridge, P., Grizzle, R., Wellman, K., Rheault, R., Steinberg, J., Jacob, A., Davenport, E. D., Ayvazian, S., Chintala, M., Tedesco, M. A. (2018). Role of Shellfish Aquaculture in the Reduction of Eutrophication in an Urban Estuary. *Environmental Science and Technology*, *52*(1), 173–183. https://doi.org/10.1021/acs.est.7b03970

9. Buchanan, J. T. (2001). In vivo transfection of adult eastern oysters *Crassostrea virginica*. *World Aquaculture Society*, *32*(3), 286–299.

10. Buchannan, J. T. (1999). Production of Transgenic Eastern Oysters. Retrieved from: *Louisiana State University and Agricultural and Mechanical College Library.* 378.76 L930D 1999 BUCH.

11. Cadoret, J. P., Debón, R., Cornudella, L., Lardans, V., Morvan, A., Roch, P., & Boulo, V. (1999). Transient expression assays with the proximal promoter of a newly characterized actin gene from the oyster Crassostrea gigas. *FEBS Letters*, *460*(1), 81–85. https://doi.org/10.1016/S0014-5793(99)01319-8

12. Carballal, M.J., Barber, B.J., Iglesias, D., Villalba, A., 2015. Neoplastic diseases of marine bivalves. J. Invertebr. Pathol. 131, 83–106.

13. Chavez-Villalba, J., Barret, J., Mingant, C., Cochard, J.C., Le Pennec, M., 2002a. Autumn conditioning of the oyster Crassostrea gigas: a new approach. Aquaculture 210, 171–186.

14. Chavez-Villalba, J., Pommier, J., Andriamiseza, J., Pouvreau, S., Barret, J., Cochard, J.-C., Le Pennec, M., 2002b. Broodstock conditioning of the oyster Crassostrea gigas: origin and temperature effect. Aquaculture 214 (1–4), 115–130.

15. Cheikh, B. Y., Travers, M. A., & Le Foll, F. (2017). Infection dynamics of a V. splendidus strain pathogenic to Mytilus edulis: In vivo and in vitro interactions with hemocytes. *Fish and Shellfish Immunology*, *70*, 515–523. https://doi.org/10.1016/j.fsi.2017.09.047

16. Cheng, T. C. 1975. Functional morphology and biochemistry of molluscan phagocytes. Ann. N.Y. Acad. Sci., 266, 343-379.

17. Chu, F. L. E., La Peyre J. F., Burreson C. S. 1993. Perkinsus marinus Infection and Potential Defense-Related Activities in Eastern Oysters, Crassostrea virginica: Salinity Effects. *Journal of invertebrate Pathology*, 62(3)226-232.

18. Davis, N. L., King, C. C., & Kourtis, A. P. (2017). Cytomegalovirus infection in pregnancy. *Birth Defects Research*, 109(5), 336–346. https://doi.org/10.1002/bdra.23601

19. Dennig, J., Duncan, E. (2002). Gene transfer into eukaryotic cells using activated polyamidoamine dendrimers. *Reviews in Molecular Biotechnology.* 90(3-4), 339-347. https://doi.org/10.1016/S1389-0352(01)00066-6

20. Dowle, M., Srinivasan, A. (2018). data.table: Extension of `data.frame`. R package version 1.11.4. https://CRAN.R-project.org/package=data.table

21. Dutertre, M., Beninger, P. G., Barillé, L., Papin, M., & Haure, J. (2010). Rising water temperatures, reproduction and recruitment of an invasive oyster, Crassostrea gigas, on the French Atlantic coast. *Marine Environmental Research*, 69(1), 1–9. https://doi.org/10.1016/j.marenvres.2009.07.002

22. Espinosa, E. P., & Allam, B. (2018). Reverse genetics demonstrate the role of mucosal C-type lectins in food particle selection in the oyster Crassostrea virginica. *Journal of Experimental Biology*, *221*(6). https://doi.org/10.1242/jeb.174094

23. Fabioux, C., Huvet, A., Le Souchu, P., Le Pennec, M., Pouvreau, S., 2005. Temperature and photoperiod drive Crassostrea gigas reproductive internal clock. Aquaculture 250 (1–2), 458 – 470.

24. Fernández-Robledo, J. A., Lin, Z., & Vasta, G. R. (2008). Transfection of the protozoan parasite Perkinsus marinus. *Molecular and Biochemical Parasitology*, *157*, 44–53.

25. Fernández-Robledo, J. A., Yadavalli, R, Allam, B, Pales Espinosa, E, Gerdol, M, Greco, S, Gomez- Chiarri, M, Stevick, R. J, Zhang, Y, Heil, C, Tracy, A. N., Bishop-Bailey, D, Metzger, M J. (2018). Health, From the raw bar to the bench: Bivalves as models for human. *Developmental and Comparative Immunology*. 92, 260-282.

26. Gárate, M., Moseman-Valtierra, S., & Moen, A. (2019). Potential nitrous oxide production by marine shellfish in response to warming and nutrient enrichment. *Marine Pollution Bulletin*, *146*, 236–246. https://doi.org/10.1016/j.marpolbul.2019.06.025

27. Gomez-Chiarri, M., Warren W.C., Guo, X., Proestou, D. (2015). Developing tools for the study of molluscan immunity: The sequencing of the genome of the eastern oyster, Crassostrea virginica. *Fish and Shellfish Immunology.* 46(1) 2-4. doi: 10.1016/j.fsi.2015.05.004.

28. Hansen, E. L. 1976. A cell line from embryos of Biomphalaria glabrata (Pulmonata): Establishment and characteristics. In: Tissue Culture: Applications in Medicine, Biology, and Agriculture. K. Maramorosch, ed. Academic Press Inc., New York. p. 75-97.

29. Hartman, R., Pales Espinosa, E., & Allam, B. (2018). Identification of clam plasma proteins that bind its pathogen quahog parasite unknown. *Fish and Shellfish Immunology, 77*, 214-221.

30. Ivanina, A. V., Borah, B., Rimkevicius, T., Macrander, J., Piontkivska, H., Sokolova, I. M., & Beniash, E. (2018). The role of the vascular endothelial growth factor (VEGF) signaling in biomineralization of the oyster crassostrea gigas. *Frontiers in Marine Science, 5*(AUG) doi:10.3389/fmars.2018.00309

31. Johnston, L. A., & Yoshino, T. P. (2001). Larval Schistosoma Mansoni Excretory–Secretory Glycoproteins (ESPs) Bind to Hemocytes of Biomphalaria Glabrata (GASTROPODA) Via Surface Carbohydrate Binding Receptors. *Https://Doi.Org/10.1645/0022-3395(2001)087[0786:LSMESG]2.0.CO;2*, *87*(4), 786–793. https://doi.org/10.1645/0022-3395(2001)087[0786:LSMESG]2.0.CO;2

32. Jones T. R., Kang I. H., Wheeler D. B., Lindquist R. A., Papallo A., Sabatini D.M., Golland P., Carpenter A. E. (2008) CellProfiler Analyst: data exploration and analysis software for complex image-based screens. BMC Bioinformatics 9(1):482 /doi: 10.1186/1471-2105-9-482. PMID: 19014601 PMCID: PMC2614436

33. Kaur, G., Dufour, J.M., (2012). Cell lines: Valuable tools or useless artifacts. *Spermatogenesis.* 2(1): 1–5.

34. Keller, J. M., Alwine, J. C. 1984. Cell: Activation of the SV40 late promoter: Direct effects of T antigen in the absence of viral DNA replication. *Cell Press*. 36(2), 381-389

35. King, W. L., Siboni, N., Williams, N. L. R., Kahlke, T., Nguyen, K. V., Jenkins, C., Dove, M., O'Connor, W., Seymour, J. R., Labbate, M. (2019). Variability in the composition of pacific oyster microbiomes across oyster families exhibiting different levels of susceptibility to OsHV-1 µvar disease. *Frontiers in Microbiology,* 10(MAR) doi:10.3389/fmicb.2019.00473

36. Klawonn, F., Jayaram, B., Crull, K., Kukita, A., & Pessler, F. (2013). Analysis of contingency tables based on generalised median polish with power transformations and non-additive models. *Health Information Science and Systems*, 1(1), 1–14. https://doi.org/10.1186/2047-2501-1-11

37. Krynska, B., Lewin-Kowalik, J., Seiron, A.L. (1998). Disturbance of the normal cell cycle by T antigens of SV40 viruses and JC cause some tumors. *Postpy higieny i medycyny doświadczalnej*. 53 (3) 237-257.

38. Larson, K., Roberson, B., & Hetrick, F. (1989). Effect of environmental pollutants on the chemiluminescence of hemocytes from the American oyster Crassostrea virginica. *Diseases of Aquatic Organisms*, *6*(1981), 131–136. https://doi.org/10.3354/dao006131

39. Li, X. N., Song, H. L., Li, W., Lu, X. W., & Nishimura, O. (2010). An integrated ecological floating-bed employing plant, freshwater clam and biofilm carrier for purification of eutrophic water. *Ecological Engineering*, *36*(4), 382–390. https://doi.org/10.1016/j.ecoleng.2009.11.004

40. Lu, J., Chen, T. T., Allent, S. K., Matsubara, T., & Burns, J. C. (1996). Production of transgenic dwarf surfclams, *Mulinia lateralis* , with pantropic retroviral vectors. *PNAS. USA. 93*, 3482–3486.

41. Maidji, E., Somsouk, M., Rivera, J. M., Hunt, P. W., & Stoddart, C. A. (2017). Replication of CMV in the gut of HIV-infected individuals and epithelial barrier dysfunction. *PLoS Pathogens*, *13*(2). https://doi.org/10.1371/journal.ppat.1006202

42. Maloy, A. P., Ford, S. E., Karney, R. C., & Boettcher, K. J. (2007). Roseovarius crassostreae, the etiological agent of juvenile oyster disease (now to be known as roseovarius oyster disease) in crassostrea virginica. *Aquaculture, 269*(1-4), 71-83. doi:10.1016/j.aquaculture.2007.04.008

43. Mann, R., 1979. Some biochemical and physiological aspects of growth and gametogenesis in Crassostrea gigas and Ostrea edulis grown at sustained elevated temperatures. J. Mar. Biol. Assoc. U. K. 59, 95–110.

44. McCormick-Ray, M. G., & Howard, T. (1990). Morphology and mobility of oyster hemocytes: Evidence for seasonal variations. *Journal of Invertebrate Pathology, 58*(2), 219-230. doi:10.1016/0022-2011(91)90066-Y

45. McNees, A. L., Harrigal, L. J., Kelly, A., Minard, C. G., Wong, C., & Butel, J. S. (2018). Viral microRNA effects on persistent infection of human lymphoid cells by polyomavirus SV40. *PLOS ONE*, *13*(2), e0192799. https://doi.org/10.1371/journal.pone.0192799

46. Mount, A. S., Wheeler, A. P., Paradkar, R. P., & Snider, D. (2004). Hemocyte-Mediated Shell Mineralization in the Eastern Oyster. *Science*, *304*(5668), 297–300. https://doi.org/10.1126/science.1090506

47. Neuwirth, E. (2014). RColorBrewer: ColorBrewer Palettes. R package version 1.1-2. https://CRAN.R-project.org/package=RColorBrewer

48. Noël, D. Boulo, V., Chagot, D., Mailhe, E., Paolucci, F., Clacies, C., Hervaud, E., Elston, E. (1991). Preparation and characterization of monoclonal antibodies against neoplastic hemocytes of Mytilus edulis (Bivalvia). *Diseases of Aquatic Organisms*, *19*(3), 51–58. https://doi.org/10.1016/0041-0101(91)90289-4

49. Onorevole, K. M., Thompson, S. P., & Piehler, M. F. (2018). Living shorelines enhance nitrogen removal capacity over time. *Ecological Engineering, 120*, 238-248.

50. Paillard, C., Ashton-Alcox, K. A., & Ford, S. E. (1996). Changes in bacterial densities and hemocyte parameters in eastern oysters, crassostrea virginica, affected by juvenile oyster disease. *Aquatic Living Resources, 9*(2), 145-158. doi:10.1051/alr:1996018

51. Pershing, A. J., Alexander, M. A., Hernandez, C. M., Kerr, L. A., Le Bris, A., Mills, K. E., Nye, J. A., Record, N. R., Scannell, H. A., Scott, J. D., Sherwood, G. D., Thomas, A. C. (2015). Slow adaptation in the face of rapid warming leads to collapse of the Gulf of Maine cod fishery. *Science*, *350*(6262), 809–812. https://doi.org/10.1126/science.aac9819

52. Poole, J.C., Andrews, L. G., Tollefsbol, T. O. (2001). Activity, function, and gene regulation catalytic subunit of telomerase (hTert). *Gene.* 269 (1-2) 1-12. https://doi.org/10.1016/S0378-1119(01)00440-1

53. Pipe, R. K. (1990). Hydrolytic enzymes associated with the granular haemocytes of the marine mussel mytilus edulis. *The Histochemical Journal, 22*(11), 595-603. doi:10.1007/BF01072941

54. Proestou, D. A., Corbett, R. J., Ben-Horin, T., Small, J. M., & Allen, S. K., Jr. (2019). Defining dermo resistance phenotypes in an eastern oyster breeding population. *Aquaculture Research,* 00, 1-33.

55. Qin, L., Pahud, D. R., Ding, Y.,Bielinska, A. U., Kukowska Latallo, J. F., Baker, J. R., Bromberg, J. S. 1998. Efficient transfer of genes into murine cardiac grafts by starburst polyamidoamine dendrimers. Human Gene Therapy. 9:553-60.

56. Ray, N. E., Henning, M. C., Fulweiler, R. W. (2019). Nitrogen and phosphorus cycling in the digestive system and shell biofilm of the eastern oyster Crassostrea virginica. *Marine Ecology Progress Series*, *621*, 95–105. https://doi.org/10.3354/meps13007

57. R Core Team (2018). R: A language and environment for statistical computing. R Foundation for Statistical Computing, Vienna, Austria. URL: https://www.R-project.org/.

58. Richards, M., Xu, W., Mallozzi, A., Errera, R. M., & Supan, J. (2018). Production of calcium-binding proteins in Crassostrea virginica in response to increased environmental CO2 concentration. *Frontiers in Marine Science*, *5*(JUN), 1–13. https://doi.org/10.3389/fmars.2018.00203

59. Ringwood, A. H., Levi-Polyachenko, N., & Carroll, D. L. (2009). Fullerene exposures with oysters: Embryonic, adult, and cellular responses. *Environmental Science and Technology*, *43*(18), 7136–7141. https://doi.org/10.1021/es900621j

60. Rinkevich, B., (2011). Cell cultures from marine invertebrates: new insights for capturing endless stemness. Mar Biotechnol.13, 345-354.

61. Saraiva, S., Freitas, V., Ozório, R., Rato, A., Joaquim, S., Matias, D., & Neves, R. (2020). Mechanistic approach for oyster growth prediction under contrasting culturing conditions. *Aquaculture*, 735105. https://doi.org/10.1016/j.aquaculture.2020.735105

62. Sievert, C. (2018) plotly for R. https://plotly-book.cpsievert.me

63. Smaal, A.C., Ferreira, J.G., Grant, J., Petersen, J.K., Strand, I., 2019. Goods and Services of Marine Bivalves. Springer Open, Switzerland.

64. Smyth, A. R., Geraldi, N. R., Peihler, M. F. (2013). Oyster-mediated benthic-pelagic coupling modifies nitrogen pools and processes. *Marine Ecology Progress Series.* 493 (23-30).

65. Tripp, M. R. (1960). Mechanisms of removal of injected microorganisms from the American oyster, *Crassostrea virginica* (Gmelin). *Biology Bulletin.*, 119 (210–223).

66. UniprotKB. (1999). UniProtKB - O94807 (O94807_HUMAN). *Uniprot.org.* https://www.uniprot.org/uniprot/O94807

67. UniprotKB/Swissprot. (1986). UniProtKB - P03081 (ST_SV40). *Uniprot.org.* https://www.uniprot.org/uniprot/P03081

68. Vasta, G. R., Cheng, T. C., & Marchalonis, J. J. (1984). A lectin on the hemocyte membrane of the oyster (Crassostrea virginica). *Cellular Immunology*, *88*(2), 475–488. https://doi.org/10.1016/0008-8749(84)90179-5

69. Vignier, J., Volety, A. K., Rolton, A., Le Goïc, N., Chu, F. L. E., Robert, R., & Soudant, P. (2017). Sensitivity of eastern oyster (Crassostrea virginica) spermatozoa and oocytes to dispersed oil: Cellular responses and impacts on fertilization and embryogenesis. *Environmental Pollution*, *225*(January), 270–282.

https://doi.org/10.1016/j.envpol.2016.11.052

70. Wang, K., del Castillo, C., Corre, E., Espinosa, E. P., & Allam, B. (2016). Clam focal and systemic immune responses to QPX infection revealed by RNA-seq technology. *BMC Genomics, 17*(1) doi:10.1186/s12864-016-2493-9

71. Welsh, D. T. Nizzoli, B., Fano, E. A., Viaroli, P. (2015). Direct contribution of clams (Ruditapes philippinarum) to benthic fluxes, nitrification, denitrification and nitrous oxide emission in a farmed sediment. *Estuarine, Coastal and Shelf Science.* 154 (84-93).

72. Wickham, H., François, R., Henry, L., Müller, K. (2018). dplyr: A Grammar of Data Manipulation. R package version 0.7.6. https://CRAN.R-project.org/package=dplyr

73. Wickham, H., Henry, L. (2018). tidyr: Easily Tidy Data with 'spread()' and 'gather()' Functions. R package version 0.8.1. https://CRAN.R-project.org/package=tidyr

74. Wickham, H. ggplot2: Elegant Graphics for Data Analysis. Springer-Verlag New York, 2016.

75. Xu, Z., Chen, H., Wang, Z., Fan, F., Shi, P., Tu, M., & Du, M. (2019). Isolation and characterization of peptides from mytilus edulis with osteogenic activity in mouse MC3T3-E1 preosteoblast cells. *Journal of Agricultural and Food Chemistry, 67*(5), 1572-1584.

76. Yang, H., Supan, J., Guo, X., & Tiersch, T. R. (2013). Nonlethal sperm colleclion and cryopreservation in the eastern oyster crassostrea virginica. *Journal of Shellfish Research, 32*(2), 429-437. doi:10.2983/035.032.0223

77. Yoshino, T.P., Bickham, U., Bayne, C.J. (2013). Molluscan cells in culture: primary cell cultures and cell lines. Can. J. Zool. 91.

78. Zu Ermgassen, P.S.E., Spalding, M.D., Blake, B., Coen, L.D., Dumbauld, B., Geiger, S., et al., (2012). Historical ecology with real numbers: past and present extent and biomass of an imperilled estuarine habitat. *Proceedings of the Royal Society London B Biological Sciences.* 279, 3393–3400.

Appendices

Appendix A. Diagram of pmax-GFP plasmid with a CMV promoter, MCS, Kanamycin resistance, and Turbo GFP gene.

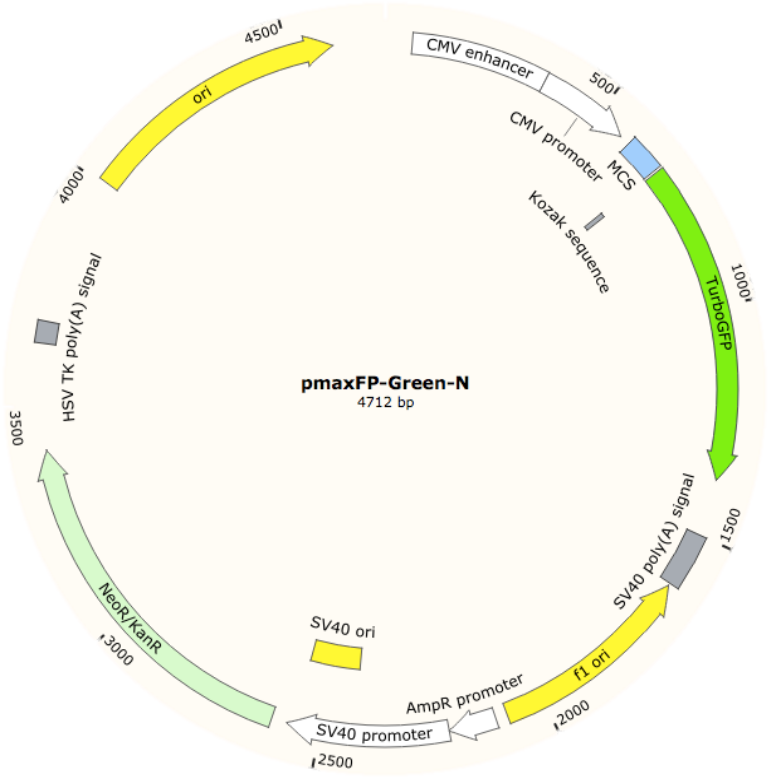

Appendix B. Diagram of pMLS-SV40-GFP with an SV40 promoter, MCS, Ampicillin resistance and GFP gene.

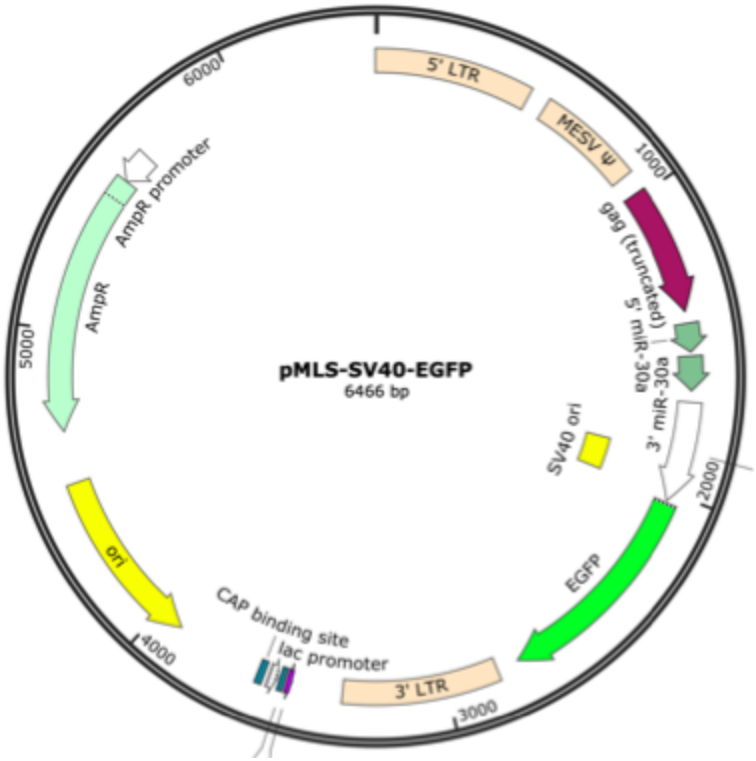

Appendix C. pmax-GFP with Actin flanking region in the MCS.

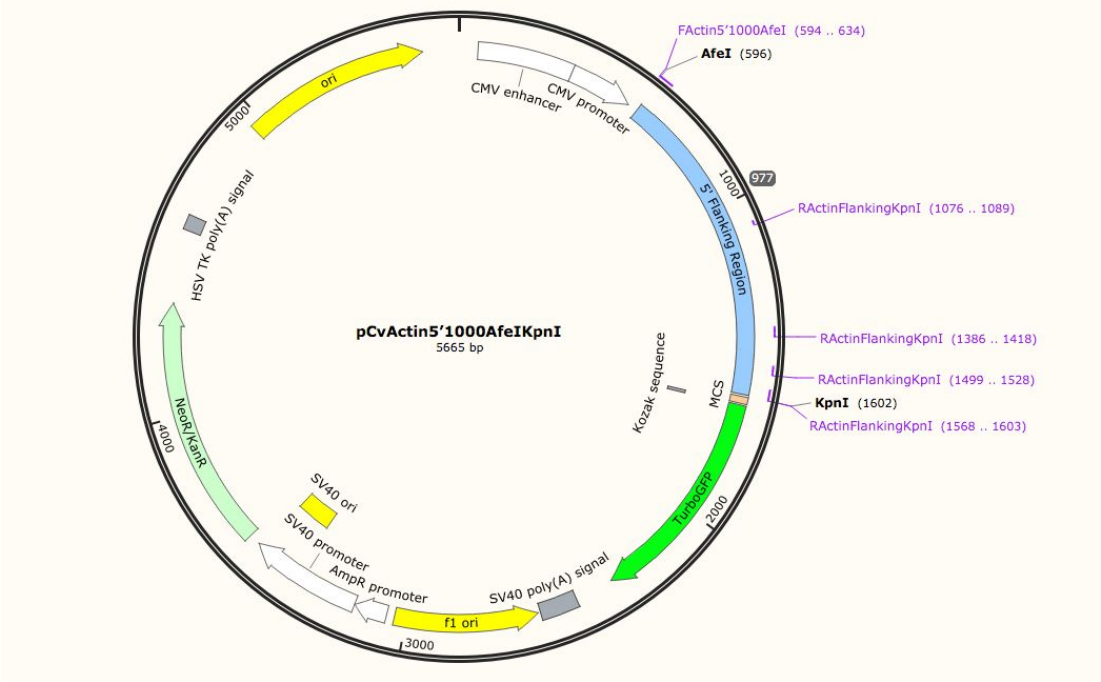

Appendix D.
Antibiotic Cocktail solution used to treat transfected oyster explants. (Buolo et al. 1996)

10 Antibiotic (10AB) stock solution.
This recipe makes up a 10X concentrated solution. The solution should be prepared in 100 mL 0.22 μm filtered seawater (FSW) and diluted 1:10 for use.
Penicillin-G 1.0 g
Streptomycin 2.0 g
Kanamycin 1.0 g
Neomycin 0.2 g
Nystatin 0.015 g
Erythromycin 0.006 g
Gentamycin 0.008 g
Polymixin-B 0.016 g
Tetracycline 0.012 g
Vancomycin 0.012 g
This recipe was published by Polne-Fuller, M. (1991) A novel technique for preparation of axenic cultures of Symbiodinium (Pyrrophyta) through selective digestion by amoebae. Journal of Phycology 27: 552-554.